The Application of Functionalized Nanocarbon Materials as Bio-interfaces in Early Diagnosis Support

A thesis submitted in fulfillment of the requirements for the degree

Master of Philosophy

By

Jie Zhao, BEng

Faculty of Engineering and IT

University of Sydney

2015

CERTIFICATION

I, Jie Zhao, declare that this thesis, submitted in fulfilment of the requirements for the award of Master of Philosophy, in the School of Chemical and Biomolecular Engineering, University of Sydney, is wholly my own work unless otherwise referenced or acknowledged. The document has not been submitted for qualifications at any other academic institution.

Jie Zhao

May, 2015

ABSTRACT

The aim of this study is to design and develop novel carbon nanotube and graphene based platforms as biosensors for electrochemically detecting dopamine. The use of such novel nanostructure, which was introduced with functional groups or bio-recognizition molecular, will enable the development of affinity-based biosensors for disease diagnostics and therapy monitoring. The electrical devices are extremely useful for dopamine determination in a fast and simple way.

In this study, a Nafion/MWCNT chip prepared by inkjet printing was developed for rapid dopamine determination in human serum. A well dispersed Nafion/MWCNT composite was investigated with homogeneous double layers which increased the efficiency of dopamine detection, producing a measurable current change at the underlying sensor electrode. This platform as described successfully demonstrated detection of dopamine concentrations (0.1 μM to 10 μM, R=0.999) using DPV and amperometry methods. This direct measurement of dopamine in serum samples without pretreatment and dilution is reported for the first time in a Nafion/MWCNT system.

In addition, to improve the specificity of the detecting probe, the direct electrochemical detection of antibody-antigen recognition was developed. Graphene can be used as an electrode surface for sensitive detection of a label. Graphene sheets were modified with gold nanoparticles or the dopamine antibody fragments (Fab') loaded with sulphur

binding with gold. Unfortunately, such bio-sensing systems did not perform sensitively and selectively for detection of the neurotransmitters/neurochemicals by utilizing certain nanostructure and introducing various functional groups. Further study will be conducted on analysing fragments' and the whole antibodies' activity and affinity of specific recognition.

ACKNOWLEDGEMENTS

Firstly, I would like to thank my supervisors Professor Andrew Harris and Associate Professor Andrew Minett for their excellent supervision and great support throughout the project. Thank you for all the opportunities you have given me and for all your help and advice over last two years. You have inspired me to be a good researcher and more importantly a better person.

I would like to thank for Tamara Church for experiment help, training and suggestions. I really appreciate the guidance Associate Professor Jun Chen has provided on all the matters about my research, as well as encouragement in the Master study. I would also like to thank Dr Joselito M. Razal, for his material provision and consulting. A special thanks to Associate Professor Weimin Zhang whose enthusiasm and attitude for science and research encourage me to pursue high degree research. I could not have done it without your support.

Thank you to all the friends and colleagues in the Laboratory for Sustainable Technology for discussion, lunch and party, making the postgraduate life more interesting. Thanks to Dr Jeffry and Ms Nancy for all technical support and advice on working and living.

Finally and most importantly, I would like to thank my family, Dad, Mum, Hua, Lei, Yali and very lovely Xuan, for your love, patience and tolerance in my whole life.

PUBLICATIONS

Jie Zhao, Yinghua Yu, Bo Weng, Weimin Zhang, Andrew T Harris, Andrew I. Minett, Zhilian Yue, Xu-Feng Huang and Jun Chen, "Sensitive and Selective Dopamine Determination in Human Serum with Inkjet Printed Nafion/MWCNT chips." Electrochemistry Communications, 2013, 37, 32-35.

Jun Chen, Roderick L. Shepherd, Joselito M. Razal, Xiao Huang, Weimin Zhang, **Jie Zhao**, Andrew T. Harris, Shu Wang, Andrew I. Minett, and Hua Zhang, "Scalable Solid-Template Reduction for Designed Reduced Graphene Oxide Architectures." ACS Applied Materials & Interfaces, 2013, 5 (16), 7676-7681.

CONFERENCE PRESENTATION

Jie Zhao, Jun Chen, Andrew Harris, Andrew Minett. Ink-Jet Printed Nafion MWCNT Chips Fabricated Bio-Electrochemical Sensors for Human Serum Dopamine Determination. The 65th Annual Meeting of the International Society of Electrochemistry, Switzerland, 2014.

ABBREVIATIONS

SPECT	photon emission computed tomography
HPLC	high performance liquid chromatography
CNT	carbon nanotube
PEG	polyethylene glycol
AuNP	Gold nanoparticle
DA	dopamine
Eox	oxidation potential
AA	ascorbic acid
UA	uric acid
SEM	scanning electron microscopy
TEM	transmission electron microscopy
XRD	X-ray diffraction

wt	weight
E_{ox}	oxidation potential
CV	cyclic voltammetry
DPV	differential pulse voltammetry
MWCNT	multi-walled carbon nanotube
I_{pa}	anodic current
I_{pc}	cathodic current
Ag	antigen
Ab	antibody
ELISA	enzyme linked immunosorbent assay
HRP	horseradish peroxidase
MB	methylene blue
LBL	layer-by-layer

ECE	electron transfer-chemical reaction-electron transfer
μ	micro
℃	degree celsius
L	litre
M	moles per litre
g	gram
cm	centimetre
nm	nanometre

Table of Contents

Certification.....I

Abstract II

Acknowledgements IV

Publications VI

Conference Presentation..... VII

Abbreviations VIII

Table of Contents XI

Table of Figures XVI

1. General introduction.....2

1.1 Motivation 2

1.2 Electrochemical biosensors 3

1.2.1 CNT based biosensor 5

1.2.2 Graphene based biosensor 7

1.2.3 Gold nanoparticle based biosensors 8

1.3 Dopamine determination sensor 10

1.4 Immobilisation techniques 11

1.5 Device fabrication 13

1.6 References 17

2. General experimental 27

2.1 Reagent and materials 27

2.2 Material preparation 28

2.2.1 Ultrasonication of CNTs 28

2.2.2 Ink-jet printing 28

2.2.3 Microwave assisted synthesis 29

2.3 Characterisation 29

2.3.1 Scanning electron microscopy 29

2.3.2 Transmission electron microscopy 30

2.3.3 X-ray diffraction 30

2.3.4 Dynamic light scattering 31

2.4 Electrochemical techniques 31

2.4.1 Cyclic voltammetry 31

2.4.2 Differential pulse voltammetry 32

2.5 References 33

3. Ink-Jet Printed Nafion/MWCNT Chips Fabricated Bio-Electrochemical Sensors for Human Serum Dopamine Determination 35

3.1 Introduction 35

3.2 Experimental 37

3.3 Results and discussions 38

3.4 Conclusions 45

3.5 References 46

4. Immunosensing Platforms Using Spontaneously Adsorbed Antibody Fragments on Gold/Graphene oxide 50

4.1 Introduction 50

4.2 Experimental 53

4.2.1 Reagents and materials 53

4.2.2 Microwave assisted synthesis of AuNP/GO 53

4.2.3 Antibody fragmentation 54

4.2.4 Antibody fragment immobilization 55

4.2.5 Characterization of electrodes 56

4.2.6 Immunosensor detection 56

4.3 Results and discussions 57

4.3.1 Design of Fab'/AuNPs/GO platform in the dopamine immunosensor 57

4.3.2 Quantitative dopamine detection with AuGO/Fab' electrode 64

4.4 Conclusions and further study 67

4.5 References 68

Table of Figures

Figure 1.1: Blood sugar testing by glucose-oxidase-based sensor [13, 14]. 4

Figure 1.2: Biosensors' elements and selected components[18]. 5

Figure 1.3: (A) Eight-electrode AuNP arrays in a single run printed by Dimatix Materials Printer; (B) Printed AuNP array with the protective polyimide insulating film; insert: building the immunoassay for electrochemical detection of human cancer biomarker [77]..... 14

Figure 1.4 Flexible printable microsensor arrays (A) and tattoo sensor (B) [80, 81]. 16

Figure 3.1: SEM images of MWCNTs (A) and Nafion/ MWCNTs (B); TEM images of MWCNTs (C) and Nafion/ MWCNTs (D). 39

Figure 3.2: DPV of 10 μM DA, 200 μM AA and 200 μM UA on the pristine MWCNT and Nafion/MWCNT electrodes. 40

Figure 3.3: (A) DPV of (a) 200 μM AA and different concentration DA (b-m: 0-10 μM) in the presence of 200 μM AA and UA mixture; (B) calibration plots of peak current to the concentration of DA. 42

Figure 3.4: Amprometry of DA (0.1, 0.2, 0.4, 0.6, 0.8, 1, 2, 4, 6, 8 & 10 μM) with/ without 200 μM AA and UA mixture; inset: calibration plots of peak current to the concentration of DA. 43

Figure 3.5: (A) DPV of DA (a-g: 0.4, 1, 2, 4, 6, 8, 10 μM) on the Nafion/MWCNT chip in undiluted human serum; (B) calibration plots of peak current to the concentration of DA. 44

Figure 4.1: Detection principles of AuNP immunosensors. The sensor surface after protein capture is shown on the left in the center. (A) The immunosensor after treatment with biotinylated Ab_2 followed by streptavidin-modified HRP resulting in HRP–Ab_2 and providing 14–16 labels per binding event. B) The immunosensor after treatment with massively labeled Ab2– methylene blue (MB)–HRP particles to obtain amplification by providing around 500000 enzyme labels per binding event as the immunosensor platform [11]. 51

Figure 4.2: Scheme of antibody fragment and immobilization on to the AuNPs. 55

Figure 4.3: (A) Optical images for gold salt solutions (top) prior to, (middle) subsequent to be heated in oil bath, and (bottom) microwave irradiation; (B) Uv-vis analysis of AuNPs synthesized in oil bath for 16h and microwave for 1h and microwave synthesized AuGO for 1h; (C) Zeta sizer test of microwave synthetized AuNPs. 59

Figure 4.4: XRD of the oil bath (A) and microwave (B) synthetized AuGO. 60

Figure 4.5: SEM images of the oil bath synthetized AuGO for 16 h with Au/GO ratio 16:1 (A&B), 2:1 (C) and 1:3 (D); the oil bath synthetized AuGO for 24 h (E) and 8 h (F) with Au/GO ratio 16:1; and microwave synthetized AuGO for 1h with Au/GO ratio 16:1 (G&H). 63

Figure 4.6: TEM images of the oil bath AuGO (A) and microwave synthetized AuNPs (B) and AuGO (C&D). 63

Figure 4.7: CV of the microwave assisted synthetized AuGO electrode (A) and AuGO/Fab' (B) in 100 μM DA solution (pH 7.0 PBS) at different scan rates (a-k): 10, 20, 40, 60, 80, 100, 120, 140, 160, 180 and 200 $mV \cdot s^{-1}$. 65

Figure 4.8: DPV of the microwave synthetized AuGO electrode (A) and AuGO-Fab' (B) in 10 (black) and 100 (red) μM DA solution (pH 7.0 PBS). 66

Chapter 1:

General Introduction

1. General introduction

1.1 Motivation

The ability to detect and quantify specific molecules, such as diagnostic proteins, drugs or environmental contaminants, plays an increasingly important role in our safety and well being. The accurate, timely and cost-effective detection of molecular targets is of great importance to applications ranging from clinical diagnostics, to environmental and food-safety monitoring, forensic identification and bio-threat detection. Taking clinical diagnostics as an example, several different experimental methods have been widely used to detect neurotransmitter released in the intact brain, such as radioimmunoassay, single photon emission computed tomography (SPECT) scans, and intracerebral dialysis method that combining with high performance liquid chromatography (HPLC) and electrochemical detection [1-4]. These traditional methods are very sensitive and specific, and utilised as clinical supports in diagnosis of neuronal system diseases. However, due to limitations of high cost, time-consumption and prerequisite of trained operators, the delay of the diagnosis and treatment may lead to irreversible result of patients' conditions. The rapid and efficient test based on point-of-care devices is therefore of the utmost importance in the field of clinical diagnostics. The electrochemical approach is one of the most promising methods for demonstrating highly specific recognition of target analytes and showing a direct signal [5]. Compared to other conventional methods, bio-electrochemical sensors show many advantages: an

extremely small device can be made to conveniently implant in vivo or directly test real samples with minor tissue damage and, because the response is fast, the neurotransmitter can be monitored in real time [6]. Indeed, despite decades of effort researchers have yet to find a general approach that adapts the versatility, specificity and affinity of the biological recognition event into user-friendly, inexpensive, and miniaturizable detection platforms. Motivated by the goal of expanding biosensors, I propose to develop the detection of a wide variety of clinical and other biologically-relevant targets.

1.2 Electrochemical biosensors

A biosensor is a device that detects the concentration of selective analytes in the sample and converts the specific biochemical reactions, mediated by isolated enzymes, immunosystems, tissues, or whole cells, into electrical, thermal, mass or optical signals [7, 8]. In this technology, the biological recognition event is transduced into an easily read output that readily signals the presence and, preferably, the amount of target present. Compared to other methods of biodetection, biosensors have many advantages such as increased assay speed, flexibility, and immediate interactive information to users. These benefits prove that biosensors are ideal for the applications in medical, environmental, public security and food safety areas [9, 10]. To date, only one portable biosensor is on the market, and little progress has been made toward the development of others that are both quantitative and reagentless. The single exception is a glucose-

oxidase-based blood sugar sensor (Figure 1.1) similar to those that were first described by Clark and Lyons in 1962 and Updike and Hicks in 1967, before becoming into widespread daily use by diabetics across the globe today [11, 12].

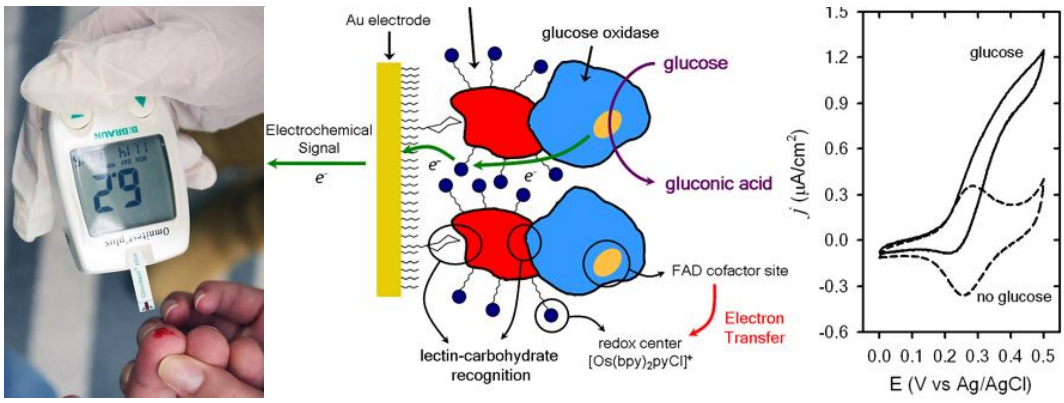

Figure 1.1: Blood sugar testing by glucose-oxidase-based sensor [13, 14].

A biosensor is generally based on the judicious and intimate coupling of the chemical or biological recognition layer that facilitates specific binding to or biochemical reaction with a target material and a physical transducer (e.g. electrode) that is used to monitor the response from the reaction. (Figure 1.2) [15, 16]. Take glucose sensors as an example, the glucose oxidase enzyme is used as a biorecognition element and the transducer is conductive substrates, such as graphene sheet, conducting polymer composites and so on. The glucose oxidase oxidizes glucose to gluconic acid and shuffles electrons into the oxygen and then reduces to hydrogen peroxide which is typically detected electrochemically [17].

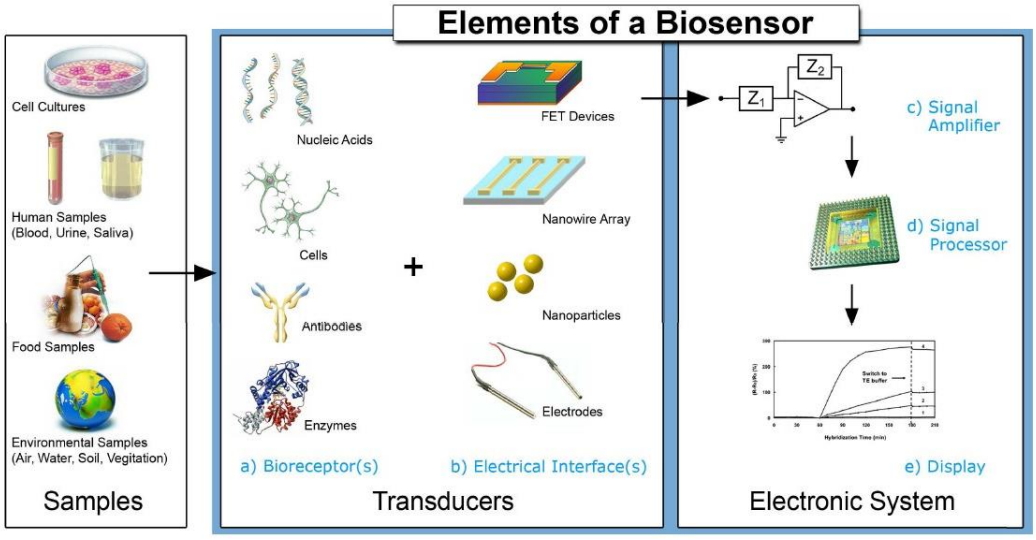

Figure 1.2: Biosensors' elements and selected components[18].

The fabrication of the transducer is a significant process to improve sensing devices' performances, especially the election of the high sensing materials coated on the signal conversion unit. The amelioration of sensitivity and selectivity have been investigated by incorporation of a variety of nanostructured materials, such as carbon nanotubes (CNTs), graphene, metal nanoparticles, magnetic nanoparticles quantum dots and so on [19-25].

1.2.1 CNT based biosensor

CNTs are a single or concentric cylindrical sp^2 carbon cylinders and this unique structure has been attracted intense research interest to explore the novel electric and

mechanical properties and applications of these materials since the discovery by Ijima in 1991 [26-28]. They offer unique properties such as enhanced electronic properties, a large edge/basal plane ratio, and rapid electrode kinetics [29-31]. Recently, CNT production has been exceeded several thousand tons per year, and CNTs and their composite materials have been used in energy storage, automotive parts, boat hulls, sporting goods, water filters, thin-film electronics, coatings, actuators and electromagnetic shields [32-34].

Currently CNTs are of interest in the building of advanced devices for small electrochemical detection applications that are sensitive to chemical and mechanical environments of the nanotubes [35]. Due to biocompatibility, bio-electrocatalytic properties, chemical functionalities, and physical stability, CNTs are applied for accumulating important bio-information (e.g. dopamine, glucose and proteins) which has been proven to enhance electrochemical reactivity and promote electron-transfer reaction of biomolecules in electrochemical detection devices [6]. For example, Joseph Wang's group reported that a three-dimensional CNT/Teflon matrix electrode was prepared for effective low-potential amperometric biosensing of glucose and ethanol, respectively, in connection with the incorporation of glucose oxidase and alcohol dehydrogenase/NAD+ [36]. This electrode overcame a major obstacle for creating CNT-based biosensing devices and expanded the scope of CNT-based electrochemical devices. Shah Ali and co-workers investigated sensitive and selective dopamine detecting using a polyaniline/Nafion/CNT based sensor [37]. The application of carbon

nanotubes greatly improved electrochemical activity of the polymer in physiological buffer, and the large surface area of the carbon nanotubes largely increased the density of the boronic acid receptors. In addition, there are some more CNT-polymer composite electrodes such as poly(vinyl acetate) deposited CNT film, polystyrene/CNT hybrids, and polyethylene glycol (PEG) chains activated CNTs have been successfully developed for simultaneous electrochemical determination [38-40]. In summary, the functionalization of CNTs by various approaches is an extremely effective to develop novel biosensors with highly selective and sensitive activity.

1.2.2 Graphene based biosensor

Graphene is a 2D single-layer graphite sheet consisting of sp^2 carbon with a honeycomb structure. Graphene sheets have been drawn attention by a number of researchers due to their interesting and exciting properties, such as high mechanical strength, high surface area (~2630 m^2 g^{-1}), sufficient porosity, superior conductivity, unique heterogeneous electron transfer and charge carrier rates, a broad potential window, rich surface chemistry, low production costs, high elasticity, and thermal conductivity [41-43]. In consideration of low cost and low environmental impact, biosensor based devices have begun to employ this conductive material in their fabrication of transduction providing electrical, electrochemical and optical signals in the sensing process [17].

Graphene has been used for electrochemical immunosensing. In immunosensing, the direct electrochemical detection of antibody-antigen recognition is usually not possible and electrochemically active labels must typically be used. There are two strategies in which graphene can be used. First, graphene can be used as an electrode surface for sensitive detection of a label [44]. This case is employed for the graphene-enhanced detection of α-fetoprotein, which is a cancer biomarker. Graphene sheets are modified with antibodies, then the α-fetoprotein is added and consequently secondary antibodies loaded with microspheres bearing horseradish peroxidase (HRP) enzyme as a sensitive label [44]. The second approach employs graphene as a label-bearing nanocarrier [45, 46]. More specifically, a gold nanoparticle electrode is modified with a probe antibody, to which phosphorylated protein is entrapped. The secondary antibody is conjugated with graphene oxide and horseradish peroxidase to generate large amounts of electroactive molecules and thus a larger signal.

1.2.3 Gold nanoparticle based biosensors

Gold nanoparticles (AuNPs) possess distinct physical and chemical attributes that make them excellent scaffolds for the fabrication of novel chemical and biological sensors [47]. Due to the ease of functionalization, AuNPs have been readily synthesized in various sizes, shape and the surrounding chemical environment. This provides a versatile platform for biological assemblies with olionucleotides, antibodies, enzymes, etc [48]. In addition, the properties like high surface-to-volume ratio and excellent

biocompatibility provide more conjugate point for biorecognition molecules. Therefore, AuNPs offer a suitable platform for selective binding and detection of biological targets in a range of biomedical application for diagnostics and therapeutic supports [49-51]. Each of these attributes of AuNPs has allowed researchers to develop novel sensing strategies with improved sensitivity, stability and selectivity. In the past decade of research, the advent of AuNP as a sensory element provided us a broad spectrum of innovative approaches for the rapid and efficient detection of metal ions, small molecules, proteins, nucleic acids, malignant cells, etc [52].

Electrochemical sensors based on AuNPs enhance electrochemical signal transduction between the receptor and the transducer, attributed to binding stability, size- and shape-related electronic properties and large surface volume. Shipway's group employed AuNP colloids to fabricate a highly sensitive and selective electrochemical sensor [53]. An AuNP/polymer based immunosensor was reported to successfully detect osteoproteogerin with detection limits of 2 pg/mL [54]. Recently Rusling et al constructed a densely packed AuNP platform combined with a multiple-enzyme labelled detection antibody bioconjugate for HIV protein determination in serum [55]. In this approach, glutathione-AuNPs were layer-by-layer assembled by electrostatic adsorption and antibodies were easily captured with the functional groups on the AuNP surface. An extension of this model using magnetic beads for easy magnetic separation and immunoreactions leads to greater signal amplification by AuNPs. This platform shows eight fold better detecting limit than their previous CNT sensor.

1.3 Dopamine determination sensor

Dopamine (DA) is one important catecholamine neurotransmitter that is produced in adrenal glands and brain and involved in brain-body integration [56]. As a potent neuromodulator, it produces effect on emotion, movement, heart rate, blood pressure, memory and so on [57]. Low levels or practically complete depletion of dopamine in the central nervous system is believed to be related to several neurological diseases, such as schizophrenia and Parkinson's disease [58]. Numerous publications have been described biosensors for some important neurotransmitter/neurochemicals, including dopamine [59].

Since electrochemical detecting of DA has been utilized as a simple analytical technique to monitor brain chemistry in the early 1970s, the researchers focus on the development of the sensitivity, selectivity as well as the low limit of detecting [60]. One of the critical issues that needs to be overcome is the overlapping or close oxidation potential (E_{ox}) of DA with co-existence compounds, particularly from the major interfering species AA (ascorbic acid) and UA (uric acid) in the nerve system [61]. Recent studies suggested that the application of electrodes based on nanomaterials like CNTs or graphene has a favourable effect on the selective sensing of DA in presence of high concentration AA or/and UA [62, 63]. These kinds of electrochemical sensing devices have highly enhanced electrochemical reactivity and promote the electron-transfer reaction of biomolecules when accumulating the important bio-information [64, 65].

Unfortunately, successful implementation of such strategies has proven elusive, due to the complex content of the unprocessed fluid samples. Up to now, there are very few reports about the DA electrochemical sensing in the serum samples without any pretreatment and dilution [66]. Previous developed DA sensor typically applied serum that was diluted in PBS buffer or even utilized pure PBS [67, 68]. The challenge of this model system is that the low DA concentration (<1 μM) decreases gradually after dilution and is out of the detecting range of the sensors [66, 69]. Furthermore, the simple PBS system fails to simulate the complex body fluid ingredients (e.g. DA, ascorbic acid, uric acid, glucose, proteins) to meet the demand of practical applications in real samples [68, 70]. Not only does oxidation of interferences produce false signal, but also serum contents are competitive to be absorbed on the electrode surface, which represses the signal transduction between DA and platform. Thus far the direct determination of DA has been set up and further studies are in urgent need for the applications of disease diagnostics and medical monitoring.

1.4 Immobilisation techniques

Nanomaterials such as gold nanoparticles, carbon nanotubes and graphene become very common in the development of electrochemical biosensor devices for important analytes such as glucose, cancer markers and drugs delivery [71]. Due to excellent biocompatibility, these nanomaterials are trended to be incorporated with bio-recognition molecules like antibodies, enzymes and DNA to improve biosensors

performance, especially specific detection, detecting limitation and stability. There are several kinds of immobilisation techniques that were employed for conjugation of antibodies with nanomaterials. Physical adsorption, chemical adsorption, and self-assembling monolayers are the most common methods onto hybrid biosensors.

Physical adsorption is the simplest way to manufacture immunosensors that are based on antibody-antigen interaction. Electrostatic adsorption of antibodies or proteins directly onto transducer surface is one of most common physical adsorption. The surface functionalised nanomaterials with positive charged ligand are associated with amino acid. The negatively charged antibodies are electrostatically adsorbed to balance the nanomaterials and maintain the charge neutrality. In this process, the simple method is to drop antibody solution on the surface by merely dipping the modified electrode. Despite of the benefit of promptness and simplicity, there are inherent shortcomings including decreased functionality and unstable bonds between biological components and conductive materials [72].

Chemical adsorption immobilisation is the covalent attachment of biorecognition substance to the transducer. This is a much stronger attachment than the physical adsorption. Linker molecules such as glutaraldehyde or carbodiimide are the common reagents involved in the chemical cross-linking. They provide binding sites at carboxy or aldehydic groups by condensation reaction. Panpan Wang et al. fabricated the electrochemical immunodevice based on antibody modified CNT paper via

glutaraldehyde cross-linking [73]. They confirmed that the cross-reactivity between antibodies and nonspecific binding at the working zones could be eliminated. Another classic example is gold-sulphur interaction which forms strong bonds with relatively high affinity of 126-146 KJ/mol [74]. It is widely applied for conjugation gold nanoparticles with biological linkers, functional groups and other molecules. Chemisorption is achieved via covalent interaction between the –SH groups of the cysteine residues or other cross-linkers and AuNP surface.

1.5 Device fabrication

Since rapid development in graphic arts and newspaper industry, printing technology has been adapted for the production of large volume electronics, for examples thin-film transistors, radio frequency identification tags, and solar cells [75]. In particular, digital inkjet printing, which has been used as a low cost research tool, is facilitating initial exploration of various aspects of printed electronics in a laboratory setting. In general, inkjet printing is a digital, non-contact printing technology that does not require an intermediate carrier for the image information deposited onto the substrate. Inkjet-printed electronics are an attractive option for the fabrication of arrays due to their relative speed of fabrication, ability to produce three-dimensional structures, and non-contact nature of the process. This allows a great deal of flexibility at the research and development stage as it does not require costly design and fabrication of specific stencils, screens or rollers.[76]. Printed patterns can be evaluated and changed rapidly at

minimal cost using simple CAD software. In addition, the availability of flat bed instruments for intermediate research, development and low volume production scale allows for transition from the laboratory bench to the production plant. Inkjet can also be made in large area and high throughput by the ganging of many print heads into large linear arrays.

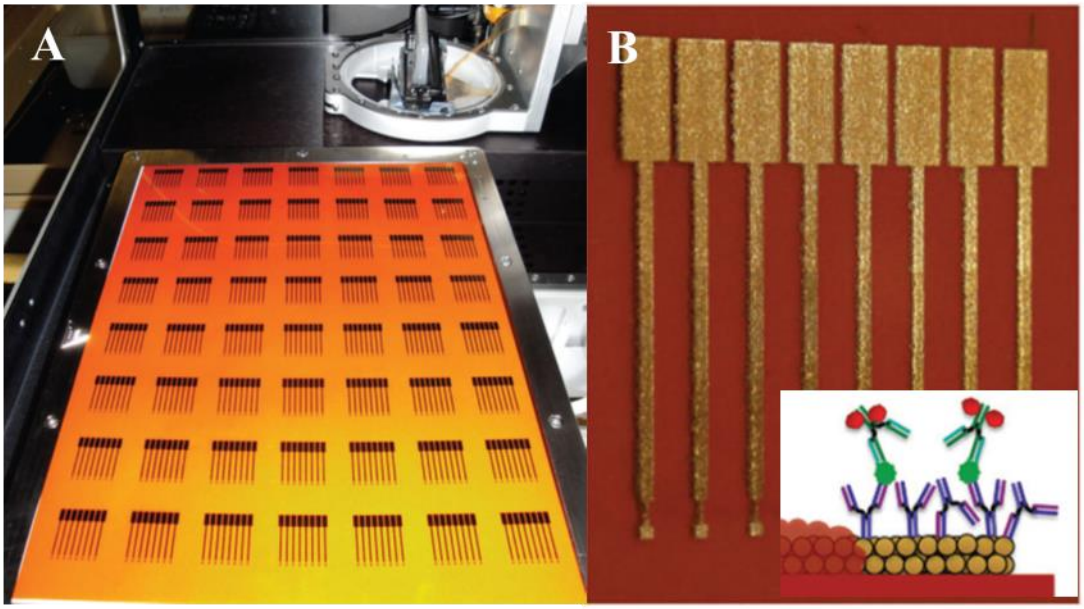

Figure 1.3: (A) Eight-electrode AuNP arrays in a single run printed by Dimatix Materials Printer; (B) Printed AuNP array with the protective polyimide insulating film; insert: building the immunoassay for electrochemical detection of human cancer biomarker [77].

Jensen and his colleagues reported the application of inkjet depositing alkyl thiols on gold in electrochemical array production for detection of cancer biomarker in serum (Figure 1.3) [77]. It offers an inexpensive non-contact fabrication method for microelectronics that is easily adapted for incorporation into sensor devices. In the inkjet printing process, the ink must meet the key requirements, such as chemical stability, particle size, excellent charge-transport, surface tension and viscosity [78]. Despite of high conductivity and good performance in sensing, the ink employed in printing must be either solute dissolved or dispersed in a solvent and pass through the nozzles without aggregation. This might be one of main limitations in the applying for printing technology in sensor fabrication [79]. In most cases, fabrication of functional device structures with inkjet printing involves the use of dilute polymer solutions. Successful application of various materials will allow a wider entry and adoption of inkjet technology. In such situations, more complicated patterns are able to be modelled and an inkjet can truly become a laboratory tool for materials discovery and device fabrication.

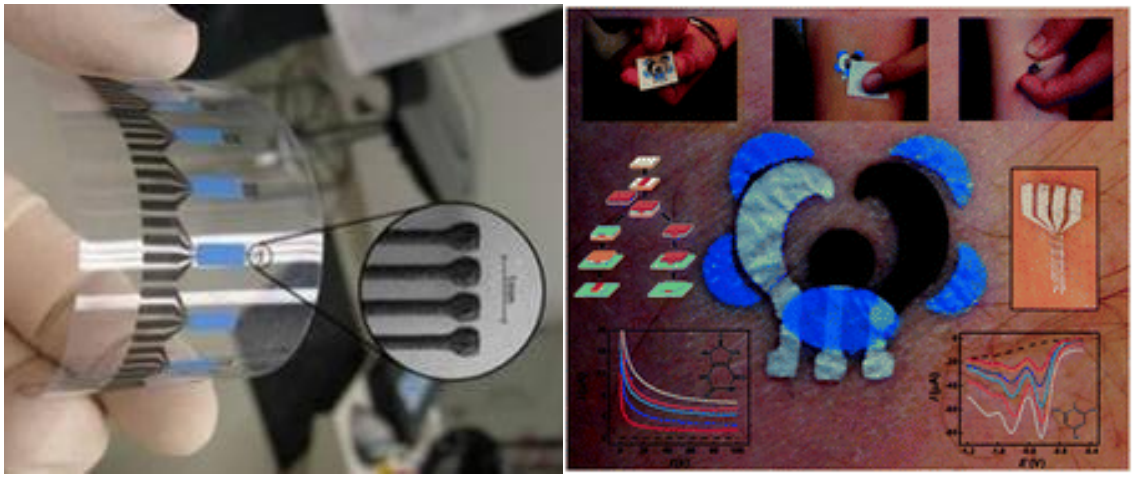

Figure 1.4 Flexible printable microsensor arrays (A) and tattoo sensor (B) [80, 81].

With continued innovation and attention to key challenges, a wide range of flexible electrochemical sensors have been developed as personal health care monitoring applications for field-based real-time monitoring of electrolytes and metabolites in sweat, tears, or saliva (Figure 1.4A) [82]. Windmiller, et al. reported a new fabrication approach combining commercially available temporary transfer tattoo paper with conventional screen printing and solid-contact polymer ion-selective electrode (ISE) methodologies (Figure 1.4B) [80]. The fabrication process was first involved printing the blue insulator ink, followed by the Ag/AgCl and the carbon inks, and finally, by another blue insulator layer. The ISE tattoos were firstly examined *in vitro* by applying them onto hard plastic substrates prior to on-body epidermal studies. The device responds rapidly to the dynamic pH changes, regaining the same potentiometric signal for a given solution pH during this continuous operation. The application of these new

series of electrochemical sensors for health monitoring of relevant compounds of physiological and security importance has leveraged conventional and widely-deployed printing techniques in conjunction with potentially commercial medical instruments.

1.6 References

1. Cheramy, A., et al., *Direct and indirect presynaptic control of dopamine release by excitatory amino acids.* Amino Acids, 1998. **14**(1-3): p. 63.

2. Innis, R., et al., *Single photon emission computed tomographic imaging demonstrates loss of striatal dopamine transporters in Parkinson disease.* Proceedings of the National Academy of Sciences, 1993. **90**(24): p. 11965.

3. Rush, R.A., P.E. Thomas, and S. Udenfriend, *Measurement of human dopamine-beta-hydroxylase in serum by homologous radioimmunoassay.* Proceedings of the National Academy of Sciences, 1975. **72**(2): p. 750.

4. Zetterström, T., et al., *In Vivo Measurement of Dopamine and Its Metabolites by Intracerebral Dialysis: Changes After d‐Amphetamine.* Journal of neurochemistry, 1983. **41**(6): p. 1769.

5. Drummond, T.G., M.G. Hill, and J.K. Barton, *Electrochemical DNA sensors.* Nature biotechnology, 2003. **21**(10): p. 1192.

6. Wang, J., *Carbon‐nanotube based electrochemical biosensors: A review.* Electroanalysis, 2005. **17**(1): p. 7.

7. Lowe, C., *Biosensors.* Philosophical Transactions of the Royal Society of London. B, Biological Sciences, 1989. **324**(1224): p. 487.

8. McNaught, A.D. and A. Wilkinson, *IUPAC compendium of chemical terminology*. Vol. 2. 1997: Blackwell Scientific Publications.

9. Rodriguez-Mozaz, S., et al., *Biosensors for environmental applications: Future development trends.* Pure and applied chemistry, 2004. **76**(4): p. 723.

10. Sadik, O., A. Wanekaya, and S. Andreescu, *Advances in analytical technologies for environmental protection and public safety.* Journal of Environmental Monitoring, 2004. **6**(6): p. 513.

11. Clark, L.C. and C. Lyons, *Electrode systems for continuous monitoring in cardiovascular surgery.* Annals of the New York Academy of Sciences, 1962. **102**(1): p. 29.

12. Updike, S. and G. Hicks, *The enzyme electrode.* Nature, 1967. **214**: p. 986.

13. Pallarola, D., et al., *Facile Glycoenzyme Wiring to Electrode Supports by Redox‐Active Biosupramolecular Glue.* Chemistry-A European Journal, 2010. **16**(47): p. 13970.

14. *Glucose sensors will be inserted to diabetic children*. 28 November 2013; Available from: http://mu-varna.bg/EN/Pages/glukozni_senzori.aspx.

15. Thévenot, D.R., et al., *Electrochemical biosensors: recommended definitions and classification.* Biosensors and Bioelectronics, 2001. **16**(1): p. 121.

16. Eggins, B.R., *Chemical sensors and biosensors*. Vol. 28. 2008: John Wiley & Sons.

17. Pumera, M., *Graphene in biosensing.* Materials Today, 2011. **14**(7): p. 308.

18. Grieshaber, D., et al., *Electrochemical biosensors-Sensor principles and architectures.* Sensors, 2008. **8**(3): p. 1400.

19. Ensafi, A.A., et al., *Highly selective determination of ascorbic acid, dopamine, and uric acid by differential pulse voltammetry using poly (sulfonazo III) modified glassy carbon electrode.* Sensors and Actuators B: Chemical, 2010. **147**(1): p. 213.

20. Xu, H.T., et al., *Simultaneous determination of dopamine and ascorbic acid with poly (3-methylthiophene)/polypyrrole bilayer-coated carbon fiber electrodes.* Analytical sciences, 1994. **10**(3): p. 399.

21. Lin, X., et al., *Electrocatalytic oxidation and determination of dopamine in the presence of ascorbic acid and uric acid at a poly (p-nitrobenzenazo resorcinol) modified glassy carbon electrode.* Sensors and Actuators B: Chemical, 2007. **122**(1): p. 309.

22. Erdogdu, G., H.B. Mark, and A.E. Karagözler, *Voltammetric Resolution of Ascorbic Acid and Dopamine at Conducting Polymer Electrodes.* Analytical Letters, 1996. **29**(2): p. 221.

23. Huang, J., et al., *Simultaneous electrochemical determination of dopamine, uric acid and ascorbic acid using palladium nanoparticle-loaded carbon nanofibers modified electrode.* Biosensors and Bioelectronics, 2008. **24**(4): p. 632.

24. Raj, C.R., T. Okajima, and T. Ohsaka, *Gold nanoparticle arrays for the voltammetric sensing of dopamine.* Journal of Electroanalytical Chemistry, 2003. **543**(2): p. 127.

25. Tian, Z.Q., et al., *Polyelectrolyte-stabilized Pt nanoparticles as new electrocatalysts for low temperature fuel cells.* Electrochemistry Communications, 2007. **9**(7): p. 1613.

26. Iijima, S., *Helical microtubules of graphitic carbon.* Nature, 1991. **354**(6348): p. 56.

27. Miao, M., *Electrical conductivity of pure carbon nanotube yarns.* Carbon, 2011. **49**(12): p. 3755.

28. Lalwani, G., et al., *Fabrication and characterization of three-dimensional macroscopic all-carbon scaffolds.* Carbon, 2013. **53**: p. 90.

29. Viry, L., et al., *Discrimination of dopamine and ascorbic acid using carbon nanotube fiber microelectrodes.* Physical Chemistry Chemical Physics, 2010. **12**(34): p. 9993.

30. Cui, H.F., et al., *Enhancement of dopamine sensing by layer-by-layer assembly of PVI–dmeOs and Nafion on carbon nanotubes.* Nanotechnology, 2010. **21**: p. 215601.

31. Kong, J., et al., *Nanotube molecular wires as chemical sensors.* Science, 2000. **287**(5453): p. 622.

32. Dalton, A.B., et al., *Super-tough carbon-nanotube fibres.* Nature, 2003. **423**(6941): p. 703.

33. Banerjee, S. and S.S. Wong, *Synthesis and characterization of carbon nanotube-nanocrystal heterostructures.* Nano letters, 2002. **2**(3): p. 195.

34. De Volder, M.F., et al., *Carbon nanotubes: present and future commercial applications.* Science, 2013. **339**(6119): p. 535.

35. Kang, I., et al., *A carbon nanotube strain sensor for structural health monitoring.* Smart materials and structures, 2006. **15**(3): p. 737.

36. Wang, J. and M. Musameh, *Carbon nanotube/teflon composite electrochemical sensors and biosensors.* Analytical chemistry, 2003. **75**(9): p. 2075.

37. Ali, S.R., et al., *A nonoxidative sensor based on a self-doped polyaniline/carbon nanotube composite for sensitive and selective detection of the neurotransmitter dopamine.* Analytical chemistry, 2007. **79**(6): p. 2583.

38. Wei, C., et al., *Multifunctional chemical vapor sensors of aligned carbon nanotube and polymer composites.* Journal of the American Chemical Society, 2006. **128**(5): p. 1412.

39. Spitalsky, Z., et al., *Carbon nanotube–polymer composites: chemistry, processing, mechanical and electrical properties.* Progress in Polymer Science, 2010. **35**(3): p. 357.

40. Liao, Y., et al., *Carbon nanotube/polyaniline composite nanofibers: Facile synthesis and chemosensors.* Nano letters, 2011. **11**(3): p. 954.

41. Lv, W., et al., *Graphene-DNA hybrids: self-assembly and electrochemical detection performance.* J. Mater. Chem., 2010. **20**(32): p. 6668.

42. Ma, J., et al., *Preparation, characterization and antibacterial properties of silver-modified graphene oxide.* Journal of Materials Chemistry, 2011. **21**(10): p. 3350.

43. Yang, X., et al., *Bioinspired Effective Prevention of Restacking in Multilayered Graphene Films: Towards the Next Generation of High - Performance Supercapacitors.* Advanced Materials, 2011. **23**(25): p. 2833.

44. Du, D., et al., *Sensitive immunosensor for cancer biomarker based on dual signal amplification strategy of graphene sheets and multienzyme functionalized carbon nanospheres.* Analytical chemistry, 2010. **82**(7): p. 2989.

45. Du, D., et al., *Functionalized graphene oxide as a nanocarrier in a multienzyme labeling amplification strategy for ultrasensitive electrochemical immunoassay of phosphorylated p53 (S392).* Analytical chemistry, 2011. **83**(3): p. 746.

46. Du, D., et al., *Multiplexed electrochemical immunoassay of phosphorylated proteins based on enzyme-functionalized gold nanorod labels and electric field-driven acceleration.* Analytical chemistry, 2011. **83**(17): p. 6580.

47. Saha, K., et al., *Gold nanoparticles in chemical and biological sensing.* Chemical reviews, 2012. **112**(5): p. 2739.

48. Yeh, Y.-C., B. Creran, and V.M. Rotello, *Gold nanoparticles: preparation, properties, and applications in bionanotechnology.* Nanoscale, 2012. **4**(6): p. 1871.

49. Daniel, M.-C. and D. Astruc, *Gold nanoparticles: assembly, supramolecular chemistry, quantum-size-related properties, and applications toward biology, catalysis, and nanotechnology.* Chemical Reviews-Columbus, 2004. **104**(1): p. 293.

50. Deng, Z.J., et al., *Plasma protein binding of positively and negatively charged polymer-coated gold nanoparticles elicits different biological responses.* Nanotoxicology, 2012(0): p. 1.

51. Zhao, W., M.A. Brook, and Y. Li, *Design of Gold Nanoparticle‐Based Colorimetric Biosensing Assays.* ChemBioChem, 2008. **9**(15): p. 2363.

52. Wilson, R., *The use of gold nanoparticles in diagnostics and detection.* Chemical Society Reviews, 2008. **37**(9): p. 2028.

53. Shipway, A., M. Lahav, and I. Willner, *Nanostructured gold colloid electrodes.* Advanced Materials, 2000. **12**(13): p. 993.

54. Singh, K., et al., *An amperometric immunosensor for osteoproteogerin based on gold nanoparticles deposited conducting polymer.* Biosensors & bioelectronics, 2008. **23**(11): p. 1595.

55. Mani, V., et al., *Ultrasensitive immunosensor for cancer biomarker proteins using gold nanoparticle film electrodes and multienzyme-particle amplification.* ACS nano, 2009. **3**(3): p. 585.

56. Jackowska, K. and P. Krysinski, *New trends in the electrochemical sensing of dopamine.* Analytical and bioanalytical chemistry, 2013. **405**(11): p. 3753.

57. Mora, F., et al., *Stress, neurotransmitters, corticosterone and body–brain integration.* Brain research, 2012. **1476**: p. 71.

58. Stone, J.M., P.D. Morrison, and L.S. Pilowsky, *Review: Glutamate and dopamine dysregulation in schizophrenia—a synthesis and selective review.* Journal of Psychopharmacology, 2007. **21**(4): p. 440.

59. Jacobs, C.B., M.J. Peairs, and B.J. Venton, *Review: Carbon nanotube based electrochemical sensors for biomolecules.* Analytica Chimica Acta, 2010. **662**(2): p. 105.

60. Adams, R.N., *Probing brain chemistry with electroanalytical techniques.* Analytical chemistry, 1976. **48**(14): p. 1126A.

61. Hou, S., et al., *Highly Sensitive and Selective Dopamine Biosensor Fabricated with Silanized Graphene.* The Journal of Physical Chemistry C, 2010. **114**: p. 14915.

62. Lange, U., N.V. Roznyatovskaya, and V.M. Mirsky, *Conducting polymers in chemical sensors and arrays.* Analytica Chimica Acta, 2008. **614**(1): p. 1.

63. Zhao, J., et al., *Carbon nanotube nanoweb–bioelectrode for highly selective dopamine sensing.* ACS applied materials & interfaces, 2011. **4**(1): p. 44.

64. Tang, Z.K., et al., *Superconductivity in 4 angstrom single-walled carbon nanotubes.* Science, 2001. **292**(5526): p. 2462.

65. Ding, R.G., et al., *Recent advances in the preparation and utilization of carbon nanotubes for hydrogen storage.* Journal of Nanoscience and Nanotechnology, 2001. **1**(1): p. 7.

66. Özcan, A. and Y. Şahin, *Selective and Sensitive Voltammetric Determination of Dopamine in Blood by Electrochemically Treated Pencil Graphite Electrodes.* Electroanalysis, 2009. **21**(21): p. 2363.

67. Goyal, R.N., et al., *Electrochemical Sensor for the Determination of Dopamine in Presence of High Concentration of Ascorbic Acid Using a Fullerene‐C60 Coated Gold Electrode.* Electroanalysis, 2008. **20**(7): p. 757.

68. Zhao, Y., et al., *Selective detection of dopamine in the presence of ascorbic acid and uric acid by a carbon nanotubes-ionic liquid gel modified electrode.* Talanta, 2005. **66**(1): p. 51.

69. Huang, J., et al., *Simultaneous electrochemical determination of dopamine, uric acid and ascorbic acid using palladium nanoparticle-loaded carbon nanofibers modified electrode.* Biosens. Bioelectron., 2008. **24**(4): p. 632.

70. Viry, L., et al., *Discrimination of dopamine and ascorbic acid using carbon nanotube fiber microelectrodes.* Phys. Chem. Chem. Phys., 2010. **12**(34): p. 9993.

71. Putzbach, W. and N.J. Ronkainen, *Immobilization techniques in the fabrication of nanomaterial-based electrochemical biosensors: A review.* Sensors, 2013. **13**(4): p. 4811.

72. Hanefeld, U., L. Gardossi, and E. Magner, *Understanding enzyme immobilisation.* Chemical Society Reviews, 2009. **38**(2): p. 453.

73. Wang, P., et al., *Paper-based three-dimensional electrochemical immunodevice based on multi-walled carbon nanotubes functionalized paper for sensitive point-of-care testing.* Biosensors and Bioelectronics, 2012. **32**(1): p. 238.

74. Louis, C. and O. Pluchery, *Gold nanoparticles for physics, chemistry and biology*2012: World Scientific.

75. Singh, M., et al., *Inkjet printing—process and its applications.* Advanced Materials, 2010. **22**(6): p. 673.

76. Weng, B., et al., *Fabrication and Characterization of Cytocompatible Polypyrrole Films Inkjet Printed from Nanoformulations Cytocompatible, Inkjet‐Printed Polypyrrole Films.* Small, 2011. **7**(24): p. 3434.

77. Jensen, G.C., et al., *Inkjet-printed gold nanoparticle electrochemical arrays on plastic. Application to immunodetection of a cancer biomarker protein.* Physical Chemistry Chemical Physics, 2011. **13**(11): p. 4888.

78. Weng, B., et al., *Gemini surfactant doped polypyrrole nanodispersions: an inkjet printable formulation.* Journal of Materials Chemistry, 2011. **21**(6): p. 1918.

79. De Gans, B.-J. and U.S. Schubert, *Inkjet printing of well-defined polymer dots and arrays.* Langmuir, 2004. **20**(18): p. 7789.

80. Windmiller, J.R., et al., *Electrochemical sensing based on printable temporary transfer tattoos.* Chemical Communications, 2012. **48**(54): p. 6794.

81. Windmiller, J.R. and J. Wang, *Wearable Electrochemical Sensors and Biosensors: A Review*. Electroanalysis, 2013. **25**(1): p. 29.

82. Bandodkar, A.J. and J. Wang, *Non-invasive wearable electrochemical sensors: a review*. Trends in biotechnology, 2014.

Chapter 2:

General Experimental

2. General experimental

2.1 Reagent and materials

Reagent name	Grade	Company
Acetone	Analytical reagent	Ajax
Ascorbic acid	Analytical reagent	Sigma
Multi-walled carbon nanotube	Thin 95% C purity	Nanocyl
Disodium hydrogen phosphate	Analytical reagent	Sigma-Aldrich
Dopamine hydrochloride	Analytical reagent	Sigma-Aldrich
Ethanol	Analytical reagent	Ajax
Gold(III) chloride trihydrate	99.999% trace metals basis	Sigma-Aldrich
Hydrochloric acid	Analytical reagent	Sigma-Aldrich
Hexane	Analytical reagent	Ajax
Nafion	5% in lower aliphatic	Fluka
Oleylamine	Analytical reagent	Ajax

Sodium chloride	Analytical reagent	Fluka
Sodium dihydrogen phosphate	Analytical reagent	Fluka
Sodium hydroxide	Analytical reagent	Fluka

2.2 Material preparation

2.2.1 Ultrasonication of CNTs

The dispersion of carbon nanotube in ethanol or water was carried out using 30W and 20Hz in the pulse method of 1 second on/ 1 second off for 1 hour. The dispersion of functionalized CNT was ultrasonicated with the same procedure for 30 minutes. The ultrasonication is Branson Digital Sonifier Model 102C.

2.2.2 Ink-jet printing

The Nafion/MWCNT chips were printed from inkjet printable Nafion/MWCNT nanodispersion by using a piezoelectric Dimatix Materials Printer (DMP 2800), equipped with a 10 pL cartridge (DMCLCP-11610) at room temperature. The

formulation was typically printed using a jet voltage of 25.0 V, a frequency of 5.0 kHz, and a customized wave-form.

2.2.3 Microwave assisted synthesis

Microwave assisted reduction of metallic salts is a relatively new reduction technique that has shown significant progress in terms of reducing the time taken to reduction compared to traditional reduction techniques [1]. Microwave assisted reduction will commonly utilise a polyol as both the solvent and the reducing agent. In this study, a microwave oven (MDS-10, Sineo Microwave Technology) with a PTFE-lined pressure vessel was applied to heat the $HAuCl_4$ solution to 90 ℃.

2.3 Characterisation

2.3.1 Scanning electron microscopy

Scanning electron microscopy (SEM) is widely used for morphological analysis of nanostructured materials. The images obtained are created through the focusing of a high energy beam of electrons via a thermionic, Schottky or field emission cathode onto the sample. In this study, a Zeiss ULTRA Plus SEM was used to monitor electrode materials. AuNPs and AuGO were placed into the vacuum system, attached on a stage

using adhesive carbon tape. Nafion-MWCNTs solution was dropped on the glassy carbon and ready to be analysed after dried in the oven.

2.3.2 Transmission electron microscopy

High resolution transmission electron microscopy (TEM) imaging was performed on a JEOL 2100 TEM. All samples were prepared for TEM by dispersion in water or hexane. The dispersions were dropped cast onto holey carbon TEM grids and dried in the fumehood prior to TEM analysis.

2.3.3 X-ray diffraction

X-ray diffraction (XRD) refers to the analysis of the crystallographic structure of the material based on the reflection of the incident x-ray radiation along lattice planes within a crystal structure. XRD is based on Bragg's Law which states that the angle of reflection is related to the distance between reflecting planes. Due to variations in lattice parameters for different chemical compounds, the angle of reflection is characteristic for the crystallographic plane of a given material. Rotation of the stage upon which the sample is mounted allowing for examination of multiple different planes within a single sample giving lattice structural information.

XRD was performed on a Shimadzu S6000 x-ray spectrometer with a copper target. Spectra were obtained between angles of 5 ° and 90 ° with typical scan speeds of 1 °/min utilised.

2.3.4 Dynamic light scattering

Dynamic light scattering is used to determine the size distribution profile of small particles in suspension or polymers in solution. This technique measures the diffusion of particles moving under Brownian motion, and converts this to size and a size distribution using the Stokes-Einstein relationship. Non-invasive back scatter technology (NIBS) is incorporated to give the highest sensitivity simultaneously with the highest dynamic size and concentration range. In this work, Malvern Nano-ZS Zetasizer dynamic light scattering instrument was used to measure the particle size and distribution of AuNPs. The AuNP nanoformulation was characterized directly after dialysis without dilution or filtration using 1 mm square quartz cuvettes.

2.4 Electrochemical techniques

2.4.1 Cyclic voltammetry

The evaluation of electron transfer process at an electrode surface was performed by cyclic voltammetry (CV). This electroanalytical technique employs repetitive triangle

waveforms that swept at a constant rate from the initial potential to vertex potential, and back to initial one and records current between the working electrode and the counter electrode versus the applied voltage. In this study, CV was employed to investigate the thermodynamical and kinetics of CNT and AuGO based electrodes in a three-electrode cell with a platinum mesh counter electrode and Ag/AgCl reference electrode. The measurements were recorded using a CHI 730C biopotentiostat (CH Instruments Inc., USA).

2.4.2 Differential pulse voltammetry

Differential pulse voltammetry (DPV) is an electrochemical measurement of redox properties of electroactive conducting samples. A rectangular pulse potential is applied and current is measured shortly before the start of each pulse and at the end of each pulse. The pulse width is set up to adjust the working time of inter level potential from an initial potential and to final one. During the pulse repeating, the potential between the working electrode and the reference electrode changes at a constant difference which is plotted to the current between the working electrode and the counter electrode. In this study, CHI 730C biopotentiostat (CH Instruments Inc., USA) was carried out for determination of DA concentration using CNT-based electrodes.

2.5 References

1. Lidström, P., et al., *Microwave assisted organic synthesis—a review*. Tetrahedron, 2001. **57**(45): p. 9225.

Chapter 3:

Ink-Jet Printed Nafion/MWCNT Chips Fabricated Bio-Electrochemical Sensors for Human Serum Dopamine Determination

Chapter 3 is revised from Jie' paper, "Sensitive and Selective Dopamine Determination in Human Serum with Inkjet Printed Nafion/MWCNT chips".

3. Ink-Jet Printed Nafion/MWCNT Chips Fabricated Bio-Electrochemical Sensors for Human Serum Dopamine Determination

3.1 Introduction

Dopamine (DA) electrochemical biosensors have received increasing attention for early diagnosis of Parkinsonism, schizophrenia, and scurvy, etc. [1, 2]. Compared to traditional clinical methods, electrochemical methods prove attractive due to simple operating processes, rapid detection and cost-effectiveness. Point-of-care results can be directly shown on a monitor by electrochemical redox of DA. Unfortunately, successful implementation of such strategies has proven elusive, and there are very few reports about DA electrochemical sensing in unprocessed serum samples [3]. Previously reported DA sensors typically applied serum diluted in PBS or even pure PBS that fail to simulate the complex serum environment (e.g. DA, ascorbic acid (AA), uric acid (UA), glucose, proteins) [4, 5]. Another challenge is that low DA concentration (< 1 μM) decreases gradually after dilution and is out of the detection range of the sensors [3, 6]. Hence, direct determination of DA remains elusive and novel sensor platforms are in urgent need for applications in disease diagnostics and medical monitoring.

Prior to real sample evaluation, DA detection should be first successfully confirmed in saline with interferences present, particularly AA (up to 114 μM) and UA (137-494 μM) that have a 10^2-10^3 higher concentration than DA and an overlapping oxidation

potential [6]. One common strategy for elelctrochemical detection of DA is to use electromaterials that are highly effective to detect target analytes with a strong electronic signal, among which carbon nanotubes (CNTs) are proving to be exceptional examples because of price, bio-electrocatalytic activity, their electronic properties and physical stability [7, 8]. To improve the detection of low concentrations of DA from interferences, two approaches have often been adopted for modifying CNT sensors: complexation with Pt/Au nanoparticles or conducting polymers to improve the electrical performance of the electrode; and incorporation of anionic groups to minimise the interference from AA and UA, achieved through chemical erosion or functionalisation of CNTs [7, 9]. Nafion, as a perfluorosulfonated cation-exchange polymer, has shown to effectively improve the selectivity of DA sensing due to its ability to attract positively charged DA molecules while rejecting anionic species [10]. Nafion also serves for solubilizing and casting the CNTs onto the electrode surface, transferring the uniform dispersion to controllable sensing film. This advantage would make it possible to fabricate CNT in novel sensor designs.

In consideration of medical applications, sensor fabrication techniques have attracted great attention, among which the inkjet printing method has been employed as a low cost tool to facilitate exploration of electronic patterns [11]. However, CNTs are neither dissolved nor well-dispersed in solvents, thereby failing to pass through the nozzles without aggregation. Introduction of conductive polymer has been one approach for enhancing the properties of CNT suspensions to achieve film homogeneity, thickness

and flocculation [12]. Therefore, the composites are able to be printed by depositing thin films on the flexible substrate, the design of which presents the possibility of disposable sensing chips that are low-cost, contamination resistant and convenient [13].

In this thesis, we have described, for the first time, inkjet printing Nafion/multi-walled CNT (MWCNT) chips and their application as a disposable platform in human serum DA determination. In order to prepare a printable formulation, we synthesized homogeneous double-layer MWCNT/Nafion that alleviates diffusion issues [10]. This proposed sensing platform presents enhanced sensitivity and selectivity in DA determination of untreated real serum samples using DPV and amperometry.

3.2 Experimental

MWCNTs (4 mg, Nanocyl) were added to Nafion water solution (10 mL, 0.05 wt%, Sigma) followed by ultrasonication (Branson Digital Sonifier Model 102C) for 30 minutes. Then the dispersion was stirred overnight until well dispersed MWCNTs were achieved. Polished glassy carbon (0.2475 cm^2, GC) electrodes were coated with 20 μL Nafion/MWCNT and dried in an oven at 60 ℃. Nafion/MWCNT chips were printed by Dimatix Materials Printer 2800 (0.8*0.8 cm^2, 15 layers) on ITO coated PET and dried in an oven at 60 ℃.

The Zeta potential of Nafion/MWCNT was measured using a Zetasizer Nano ZS (Malvern Instruments). The surface morphology of electrodes was examined by a SEM (JSM7500FA, JEOL) and TEM (JEM2011, JEOL). Cyclic voltammetry (CV) and differential pulse voltammetry (DPV) were conducted on a CHI720C electrochemical workstation (CH Instruments Inc.). Amprometry was investigated using a Princeton G model 283 workstation (Princeton Applied Research). All electrochemistry measurements were conducted at room temperature with Nafion/MWCNT working electrode, Pt counter electrode and Ag/AgCl reference electrode. Phosphate buffered saline (PBS, Chem-supply, pH 7.0) was freshly prepared and human serum was purchased from Sigma-Aldrich.

3.3 Results and discussions

Untreated MWCNTs are highly hydrophobic and difficult to form a uniform dispersion in aqueous media even after extended ultrasonication. To facilitate the dispersion of MWCNTs in aqueous environment, Nafion was introduced with a mass ratio of Nafion/MWCNT ranging from 2:4 to 10:4. When the mass ratio was above 5:4, well dispersed suspensions of MWCNTs were achieved, with a high zeta potential of -68.6 mV and stability for more than 3 months with no sign of precipitation. In consideration of both low surfactant introduction and high dispersing stability, the Nafion/MWCNT composite with the ratio of 5:4 was utilized to prepare the electrode. In addition,

uniform films were produced by casting dispersions on a GC electrode, while significant aggregation took place upon drying pristine MWCNT suspension.

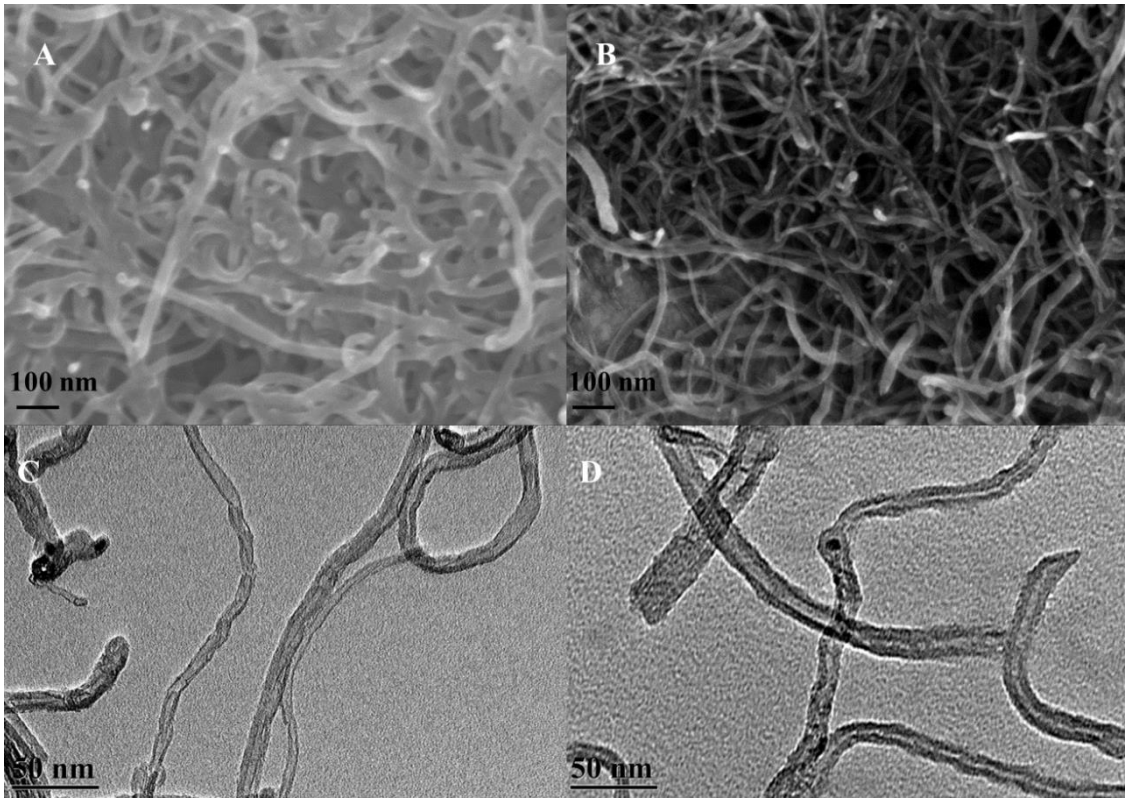

Figure 3.1: SEM images of MWCNTs (A) and Nafion/ MWCNTs (B); TEM images of MWCNTs (C) and Nafion/ MWCNTs (D).

The morphology of Nafion/MWCNT electrodes was examined using SEM. Compared to pristine MWCNTs, no significant disruption of MWCNTs was observed in the SEM and TEM micrographs of Nafion/MWCNT coated electrode, indicating that this non-covalent method retained the MWCNT pristine structure [14]. Both electrodes showed

porous network structures on the surface; however, pristine MWCNTs coated electrodes contained more aggregated bundles and ropes (Figure 3.1A&B). Such aggregation was greatly reduced by the introduction of Nafion. The main reason is probably that nanotubes, due to the negative surface molecules, are able to preclude each other by electrostatic repulsion, inducing a debundled nanostructure. On a closer look by TEM, nanotubes in the Nafion/MWCNT exhibited a bi-layered structure with inner MWCNT coated with an outer layer of Nafion, and the thickness range of the Nafion layer is approximately 5-6 nm (Figure 3.1C&D).

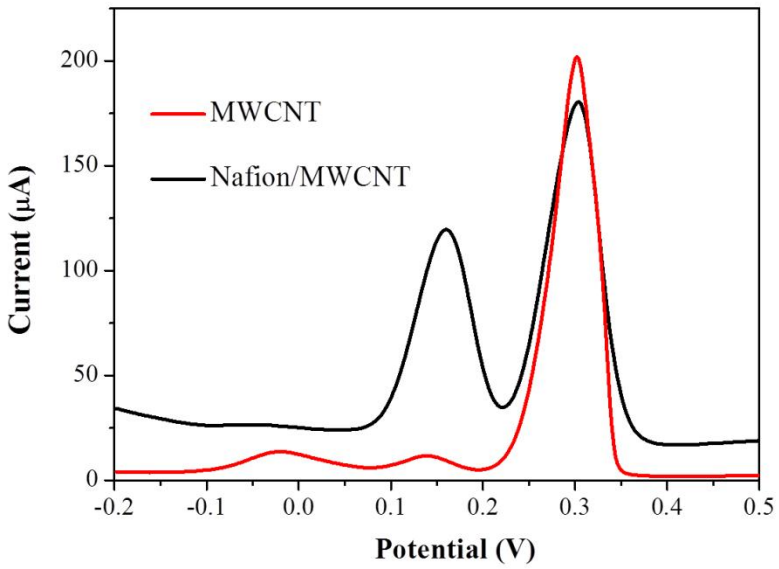

Figure 3.2: DPV of 10 μM DA, 200 μM AA and 200 μM UA on the pristine MWCNT and Nafion/MWCNT electrodes.

In order to illustrate the effect of Nafion functionalisation on the sensing activity, two electrodes, modified with either pristine MWCNTs or Nafion/MWCNTs, were prepared for DA sensing under identical testing conditions. Nafion is commonly believed to efficiently improve the interaction between DA and the electrode because of protons on sulfonic acid groups that easily transfer from one acid site to another and thus form negatively charged $-SO_3^-$ in PBS solution [15]. In DPV measurements, high DA signals were obtained at Nafion/MWCNT electrodes at 99 μA (over 12 times of unmodified electrode responses), accompanied with negligible AA response, while approximately 9.8 and 8.1 μA current was detected for 200 μM AA and 10 μM DA on the pristine MWCNT electrode (Figure 3.2). Fortunately, three peaks (around -0.02, 0.15 and 0.30 mV *vs*. Ag/AgCl for AA, DA and UA, respectively) separate well from each other, making it possible to study the DA process from interferences. Indeed, the new electrode provides a significant impact on sensing DA and impeding AA & UA. Thus, we have achieved sensitivity and selectivity improvement by coating the electrode with negatively charged, highly uniform and porous Nafion/MWCNT.

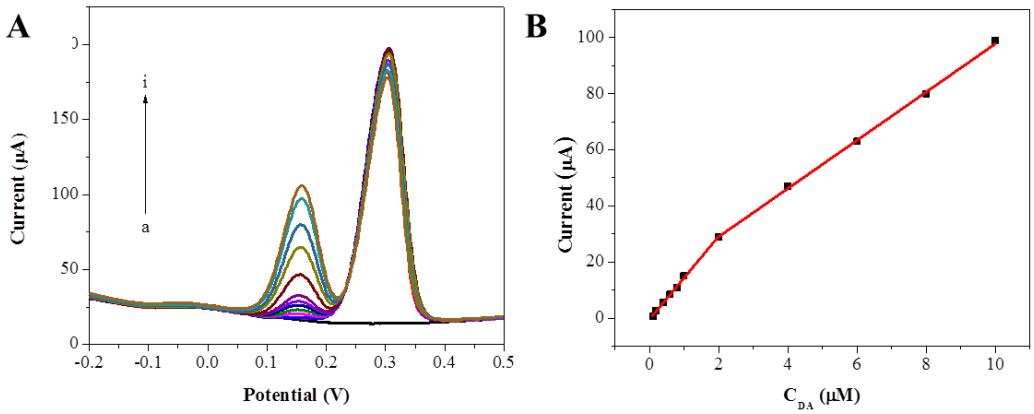

Figure 3.3: (A) DPV of (a) 200 μM AA and different concentration DA (b-m: 0-10 μM) in the presence of 200 μM AA and UA mixture; (B) calibration plots of peak current to the concentration of DA.

To demonstrate this capability of low concentration DA determination, DPV were employed as highly sensitive methods to detect responding ranges on Nafion/MWCNT electrodes in PBS. As shown in Figure 3.3A, DPV curves record the target oxidation and electron transfer processes in different solutions containing 200 μM AA, 200 μM UA and various concentration DA (0-10 μM). Peak currents for DA oxidation increase linearly as bulk concentrations of DA in the solution. This linear relationship is represented by I_{pa}=14.8C_{DA}-0.50 (R=0.999, C_{DA}: 0.1-2 μM) & I_{pa}=8.6C_{DA}+11.8 (R=1, C_{DA}: 2-10 μM) (Figure 3.3B). Consistent with high, separated and linear signal gain, this Nafion/MWCNT electrode performed exceptionally well as a detector of DA at submicromolar concentration, even with a detection limit as low as 0.1 μM.

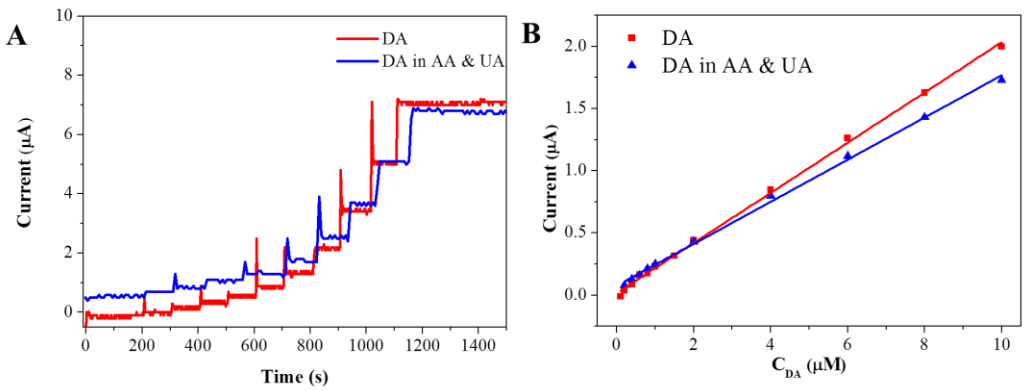

Figure 3.4: Amprometry of DA (0.1, 0.2, 0.4, 0.6, 0.8, 1, 2, 4, 6, 8 & 10 μM) with/ without 200 μM AA and UA mixture; inset: calibration plots of peak current to the concentration of DA.

In addition, amperometry method presents i-t curves at 0.2 V *vs*. Ag/AgCl resulting from successive addition of DA into PBS in a wide range of DA concentration from 0.2-10 μM (Figure 3.4A). The current reached a stable step immediately after each DA addition in PBS with/ without AA and UA in a set of measurements. Moreover, the coexistance of AA and UA never interferes with the DA oxidation or electron transfer on the surface of the electrode. We attribute this to the effective and efficient catalytic property of the electrode and selectivity of Nafion/MWCNTs to the DA oxidation at specific voltage. Furthermore, the linear relationships between oxidation currents and DA concentration were obtained from 0-10 μM DA (Figure 3.4B). The linear equations

are present as I_{pa}=0.20C_{DA}+0.017 (R=0.999) in PBS & I_{pa}=0.17C_{DA}+0.076 (R=0.999) in PBS with 200 μM AA and UA, with a detection limit of 0.2 μM DA. It was found the current responses for same concentration DA were quite similar in both cases and DA measurements are reliable using amperometry determination in Nafion/MWCNT platform.

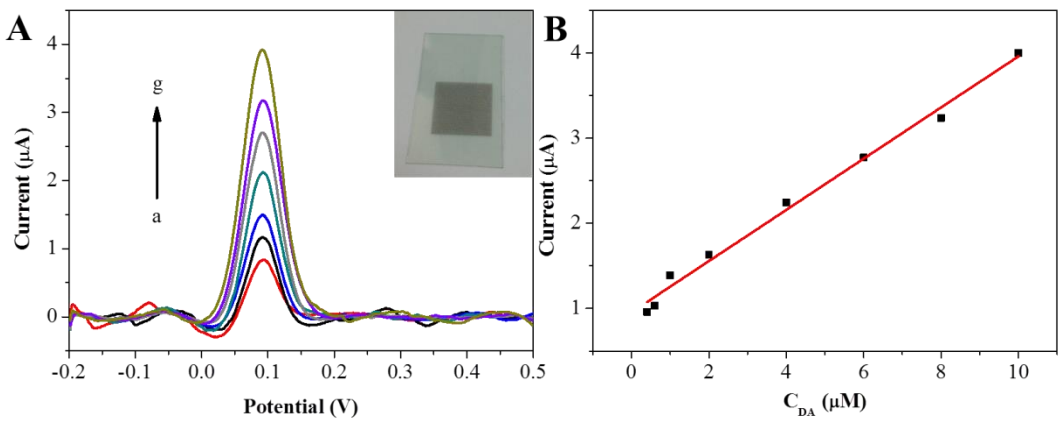

Figure 3.5: (A) DPV of DA (a-g: 0.4, 1, 2, 4, 6, 8, 10 μM) on the Nafion/MWCNT chip in undiluted human serum; (B) calibration plots of peak current to the concentration of DA.

For investigating the applicability of the proposed material, Nafion/MWCNT dispersion was inkjet printed on PET substrates as disposable sensing chips (Figure 3.5 inset). With an interest in practical applications, the printed chip was directly applied to detect DA content of real serum samples using DPV. A study was conducted utilizing healthy

human serum without any pretreatments and dilution. This method overcomes the drawback that the low concentration DA is diluted and can not reach the detection limit in the analytical system. Firstly, blank serum samples were tested in the same procedure as PBS system. No DA was found and fortunately, complex blood ingredients did not appear to interfere with the test procedure [5]. Subsequently, the method was applied to DA determination in undiluted sample with addition of different concentration DA (Figure 3.5A). The significant signals for DA were obtained with separation of serum background peaks. The linear equations are present as I_{pa} =0.30C_{DA}+0.96, with the linear relative coefficient of 0.995 and a detection range of 0.4-10 μM (Figure 3.5B). 5 chips were utilized to detect DA and the mean error is lower than 10%. This result confirms that the Nafion/MWCNT sensing is suitable to detect submicromolar DA in real samples. The direct DA detection in undiluted serum samples has for the first time been reported in a Nafion/MWCNT platform. Such satisfactory chips would provide an appropriate and sufficient strategy for the determination of DA in real samples with high sensitivity and selectivity.

3.4 Conclusions

In summary, a disposable Nafion/MWCNT chip has been successfully printed and applied to a sensitive and selective electrochemical sensor for DA determination in the presence of an excess of AA and UA in human serum. The simply fabricated platform not only resolved the overlapped current peaks of DA into other interferences, but also

achieved a dramatic electrocatalytic effect on the oxidation of DA by enhancing current signals. A widely linear relationship of DA signal against concentration was obtained from 0.1 μM to 10 μM, being free of interference from excess AA and UA. The chip was further applied in healthy human serum without any pretreatments and dilution and the satisfactory result was obtained. The simple equipment, ease of preparation and low cost of Nafion/MWCNT chips also demonstrates commercial potential in fabricating the sensor for point of care DA determination.

3.5 References

1. Savitt, J.M., V.L. Dawson, and T.M. Dawson, *Diagnosis and treatment of Parkinson disease: molecules to medicine.* J. Clin. Invest., 2006. **116**(7): p. 1744.

2. Iversen, S.D. and L.L. Iversen, *Dopamine: 50 years in perspective.* Trends Neurosci., 2007. **30**(5): p. 188.

3. Özcan, A. and Y. Şahin, *Selective and Sensitive Voltammetric Determination of Dopamine in Blood by Electrochemically Treated Pencil Graphite Electrodes.* Electroanal., 2009. **21**(21): p. 2363.

4. Goyal, R.N., et al., *Electrochemical Sensor for the Determination of Dopamine in Presence of High Concentration of Ascorbic Acid Using a Fullerene‐C60 Coated Gold Electrode.* Electroanal., 2008. **20**(7): p. 757.

5. Zhao, Y., et al., *Selective detection of dopamine in the presence of ascorbic acid and uric acid by a carbon nanotubes-ionic liquid gel modified electrode.* Talanta, 2005. **66**(1): p. 51.

6. Huang, J., et al., *Simultaneous electrochemical determination of dopamine, uric acid and ascorbic acid using palladium nanoparticle-loaded carbon nanofibers modified electrode.* Biosens. Bioelectron., 2008. **24**(4): p. 632.

7. Cao, X.H., et al., *Amperometric sensing of dopamine using a single-walled carbon nanotube covalently attached to a conical glass micropore electrode.* Electrochem. Commun., 2010. **12**(4): p. 540.

8. Lynam, C., et al., *Carbon nanotube-based transducers for immunoassays.* Carbon, 2009. **47**(10): p. 2337.

9. Zhao, J., et al., *Carbon nanotube nanoweb-bioelectrode for highly selective dopamine sensing.* ACS Appl Mater Interfaces, 2012. **4**(1): p. 44.

10. Hou, S., et al., *Highly Sensitive and Selective Dopamine Biosensor Fabricated with Silanized Graphene.* J. Phys. Chem. C, 2010. **114**(35): p. 14915.

11. Okimoto, H., et al., *Tunable Carbon Nanotube Thin-Film Transistors Produced Exclusively via Inkjet Printing.* Adv. Mater., 2010. **22**(36): p. 3981.

12. Denneulin, A., et al., *The influence of carbon nanotubes in inkjet printing of conductive polymer suspensions.* Nanotechnology, 2009. **20**(38): p. 385701.

13. Weng, B., et al., *Fabrication and Characterization of Cytocompatible Polypyrrole Films Inkjet Printed from Nanoformulations Cytocompatible, Inkjet‐Printed Polypyrrole Films.* Small, 2011. **7**(24): p. 3434.

14. Yurekli, K., C.A. Mitchell, and R. Krishnamoorti, *Small-angle neutron scattering from surfactant-assisted aqueous dispersions of carbon nanotubes.* J. Am. Chem. Soc., 2004. **126**(32): p. 9902.

15. Cui, H.F., et al., *Enhancement of dopamine sensing by layer-by-layer assembly of PVI-dmeOs and Nafion on carbon nanotubes.* Nanotechnology, 2010. **21**(21): p. 215601.

Chapter 4:

Immunosensing Platforms Using Spontaneously Adsorbed Antibody Fragments on Gold/Graphene oxide

4. Immunosensing Platforms Using Spontaneously Adsorbed Antibody Fragments on Gold/Graphene oxide

4.1 Introduction

The first immunoassay using radioactively labelled antigens (Ag) or antibodies (Ab) was reported for human insulin sensing by Yalow and Berson in 1959 [1]. Then Engvall and Perlmann described a new method known as enzyme linked immunosorbent assay (ELISA) that involved immune responses stimulate by components of the immune system and chemicals in the body [2]. As a fundamental analytic tool, ELISA is widely used to identify a substance in research work in the lab, medical diagnosis (such as HIV test and pregnancy test), toxicology, as well as industrial application (quality control and allergen detection) [3-5]. The high sensitivity (>99%) and high specificity (>99%) is attributed to high specificity of the Ab/Ag interaction and this principle has been used to develop a diverse range of immunodevices. The immunosensor, as a biosensor based on this specific interaction, incorporates biological recognition to a transducer with signal generation. In this case, the electrochemical detection, such as potentiometry, amperometry and impedimetry, monitors a variation in electrochemical signal output caused by specific binding event between the antibody and the target analyte. The aim is to develop rapid, low-cost and user-friendly point-of-care approaches for the quantitative detection of analytes, allowing frequent testing and narrowing the delay between diagnosis and treatment, and improving the penetration of molecular

diagnostics [6]. Early work on immunosensors has been reviewed (Hock, 1997) and there are more recent reviews (Cosnier, 2005, Diaz-Gonzalez et al., 2005, Rodriguez-Mozaz et al., 2006 and Centi et al., 2009) [7-10].

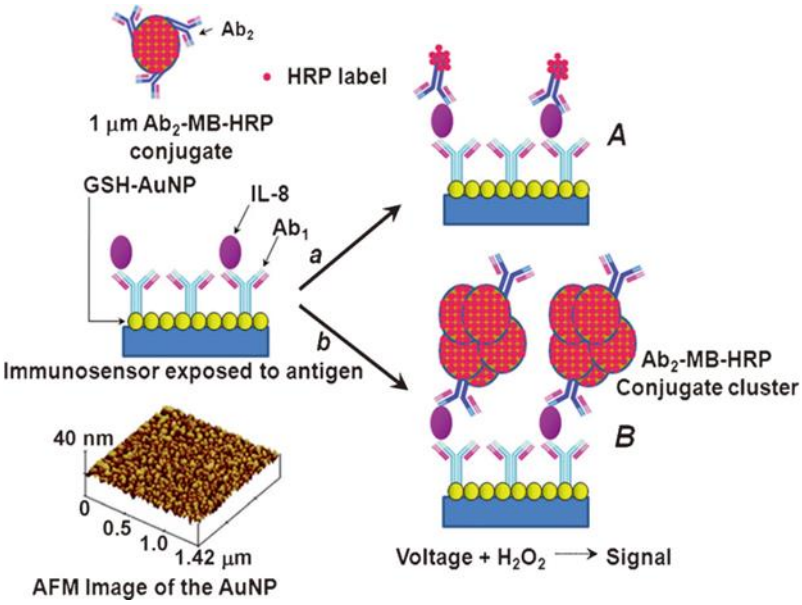

Figure 4.1: Detection principles of AuNP immunosensors. The sensor surface after protein capture is shown on the left in the center. (A) The immunosensor after treatment with biotinylated Ab_2 followed by streptavidin-modified HRP resulting in HRP–Ab_2 and providing 14–16 labels per binding event. B) The immunosensor after treatment with massively labeled Ab2– methylene blue (MB)–HRP particles to obtain amplification by providing around 500000 enzyme labels per binding event as the immunosensor platform [11].

In addition to specific detection of analytes, the introduction of nanotechnologies and fabrication of transducers have led to the development of high performance immunosensor with scope for miniaturisation, great capabilities for simultaneous analyte analysis and high-throughput screening [12]. A sensitive, stable and reproducible human chorionic gonadotropin sensors was reported with assemble layer-by-layer construction using gold nanoparticles and methylene blue [13]. The large surface area provided by the nanoparticles increases the immobilization amount of antibody and sensitivity. Rusling and his colleagues described a microfluidic device showing 8-electrode array coated with the layer-by-layer (LbL) alternate electrostatically adsorbed antibody-loaded magnetic nanoparticles on each electrode [11, 14]. Target proteins in serum are captured off-line by a heavily HRP (horseradish peroxidase) labelled antibody-magnetic particle to form antigen-bead bioconjugate that are separated from the sample magnetically and washed to remove non-specifically bound interferences. The flow is stopped to capture the particles on the electrodes. Then, antigen-magnetic particle complexes are injected into the device, and signals developed by resuming flow as well as injecting mediator and hydrogen peroxide

The aim of this chapter is to investigate the immobilisation of anti-dopamine antibody fragments into the AuNPs/GO coated electrode and the application of this immunosensor for substance detection. Antibody fragments are providing valuable alternatives to full-length Abs for new biosensing devices because they provide small, stable, highly specific reagents against the target antigen [15]. The electrochemical

properties of sensing platform will be evaluated by CV and DPV. It is now possible to produce antibody fragments with a high specificity for their target analyte and for a much wider range of uses than available with naturally formed antibodies.

4.2 Experimental

4.2.1 Reagents and materials

All reagents utilised for these chapter were analytical grade unless stated. The anti-dopamine antibody was obtained from ABCAM and stored in -20 ℃ freezer. Pepsin (sigma) was stored at 4 ℃ prior to use. Acetate buffer was fresh prepared by mixing 0.1M acetic acid and 0.1M sodium acetate and adjusted to PH 4.6. All solutions were prepared using 18MΩ·cm^{-1} deionised water.

4.2.2 Microwave assisted synthesis of AuNP/GO

GO was produced by Hummers's method and purified using a freezing dryer [16]. As-synthesized GO (0.05 mg/mL) was added to ethanol and hexane mixture (the ratio is 2:23) including 4 mM $HAuCl_4$ and 140 mM oleylamine. After stirred for 1 minute, the solution was sealed in a PTFE-lined pressure vessel in a microwave oven (MDS-10, Sineo Microwave Technology), heated to 90 ℃ and held at that temperature for 1 hour. The vessel was left overnight at room temperature and then the solution was centrifuged

at 6000 rpm for 15 minutes to collect AuNP/GO composites. In the oil bath synthesis method, the 0.05 mg/ml GO mixture described above was heated to 60 ℃ for 16 hours and obtained after centrifugation for three times.

4.2.3 Antibody fragmentation

Fab' fragments of anti-dopamine antibody were used instead of the whole antibody. The first involved splitting the antibody into $F(ab')_2$ fragments and then cleaving them into Fab'. Prior to digestion the antibody (1 mg/ml) was diluted ten times by 0.2 M acetate buffer (pH 4.6). An equal volume of pepsin solution was prepared in the same buffer with an enzyme/antibody ratio of 1:20. Then three groups of the mixture were shaken in a 37 ℃ incubator for 1, 4 and 12 hours. As each group is removed, 2M Triz base was added to adjust pH to neutral to stop the reaction [17]. The antibody was cleaved into one $F(ab')_2$ fragment and numerous small peptides of Fc portion. The reduction of $F(ab')_2$ was prepared as protocol [18]. Equal volume of 2-MEA in 0.1M PBS (pH 7.2) was added to $F(ab')_2$ solution and the mixture was incubated at 37 ℃ for 1 hour. Followed by centrifugation at 6000 rpm, the fragments were washed by PBS buffer for 3 times and collected in 0.5 ml Eppendorf tube.

4.2.4 Antibody fragment immobilization

The immobilization procedure was performed on a glassy carbon disk electrode that was coated with AuGO, after the antibodies were cleaved into Fab' fragments (Figure 4.2). The GC was polished by aluminium powder, followed by coating with 10 µl AuGO. After the electrode dried in the fumehood, 10 µl antibody fragments of a concentration of 0.1 mg/ml was loaded to AuGO and incubated for 12 hours at 4 °C. The Fab' immobilized electrode was ready to use after rinsed thoroughly with Milli-Q water to remove unreactive fragments.

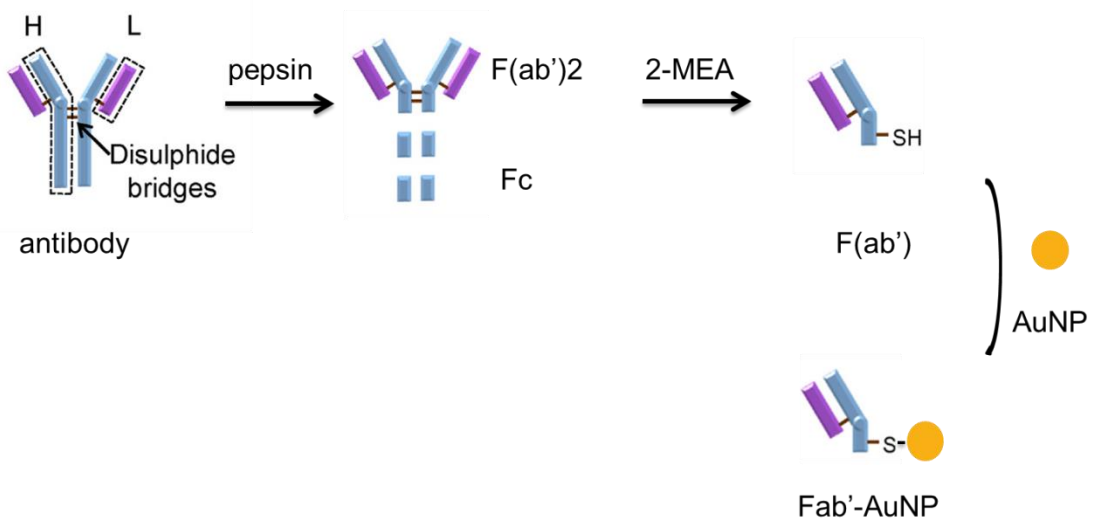

Figure 4.2: Scheme of antibody fragment and immobilization on to the AuNPs.

4.2.5 Characterization of electrodes

The Zeta potential of AuNPs was measured using a Zetasizer Nano ZS (Malvern Instruments). Electrodes' surface morphology was examined by an X-ray diffraction (XRD, S6000, Shimadzu), scanning electron microscopy (SEM, ULTRA Plus, Zeiss) and transmission electron microscopy (TEM, JEM2100, JEOL).

4.2.6 Immunosensor detection

Cyclic voltammetry (CV) was used to test the electrochemical performance of the AuGO electrode with or without antibody fragment immobilization. The working electrode in the system was recorded at different scan rates range from 20 to 200 $mV \cdot s^{-1}$, respectively. The determination of the dependence of DA concentration on the electrochemical response was obtained using DPV method. The parameters used to record DPV are as follows: 0.05 V for the amplitude, 0.05 s for the pulse width, 0.025 s for the sample width, and 0.2 s for the pulse period, respectively. A CHI760C electrochemical workstation (CH Instruments Inc., USA) was utilized to perform all the electrochemical measurements. All measurements were conducted at room temperature in a standard three-electrode cell that consists of an AuGO/Fab' working electrode, a Pt mesh counter electrode and an Ag/AgCl reference electrode.

4.3 Results and discussions

4.3.1 Design of Fab'/AuNPs/GO platform in the dopamine immunosensor

The optical colour change observed for gold during oil bath or irradiation of the salt (in this case without the presence of GO) can be seen in

Figure 4.3A. The observed colour change from yellow to pink for the $HAuCl_4$/oleylamine/hexane solution, with microwave stimulation, is characteristic of the formation of gold nanoparticles. The formation of a black mixture solution in oil bath corresponds to the reduction of $AuCl_4^-$ as well. This confirms there are larger (micro) gold particles in solution after heating for the metal.

UV-Visible spectroscopy is applied to measure the AuNPs' surface plasmon resonance and investigate properties, such as nanoparticle size, concentration, and aggregation level [19]. All samples synthesized in either oil bath or microwave oven were tested by uv-vis, which provided preliminary analysis of the successful presence of AuNPs in the solution in a short time (Figure 4.3). In the oil synthesis method, a peak appears in the UV-Visible spectrum at around 530 nm in the sample heated for 16 hours, while 1 hour, 4 hours and 8 hours solutions did not show apparent gold uv absorption in the range from 350 to 1000 nm. Compared to the traditional method, microwave assisted synthesis is a more efficient way to produce AuNPs. The nanoparticles formed in one

hour's microwave inradiation in both cases with GO incorporation or not. The presence of gold nanoparticle and GO sheet is also confirmed crystalline nature analysis by the XRD tests (Figure 4.4). Furthermore, the particle size distribution was measured by zetasizer and the analysis and characterization of AuNPs (1 h microwave) shows the size is around 3 d.nm of 99.7% volume.

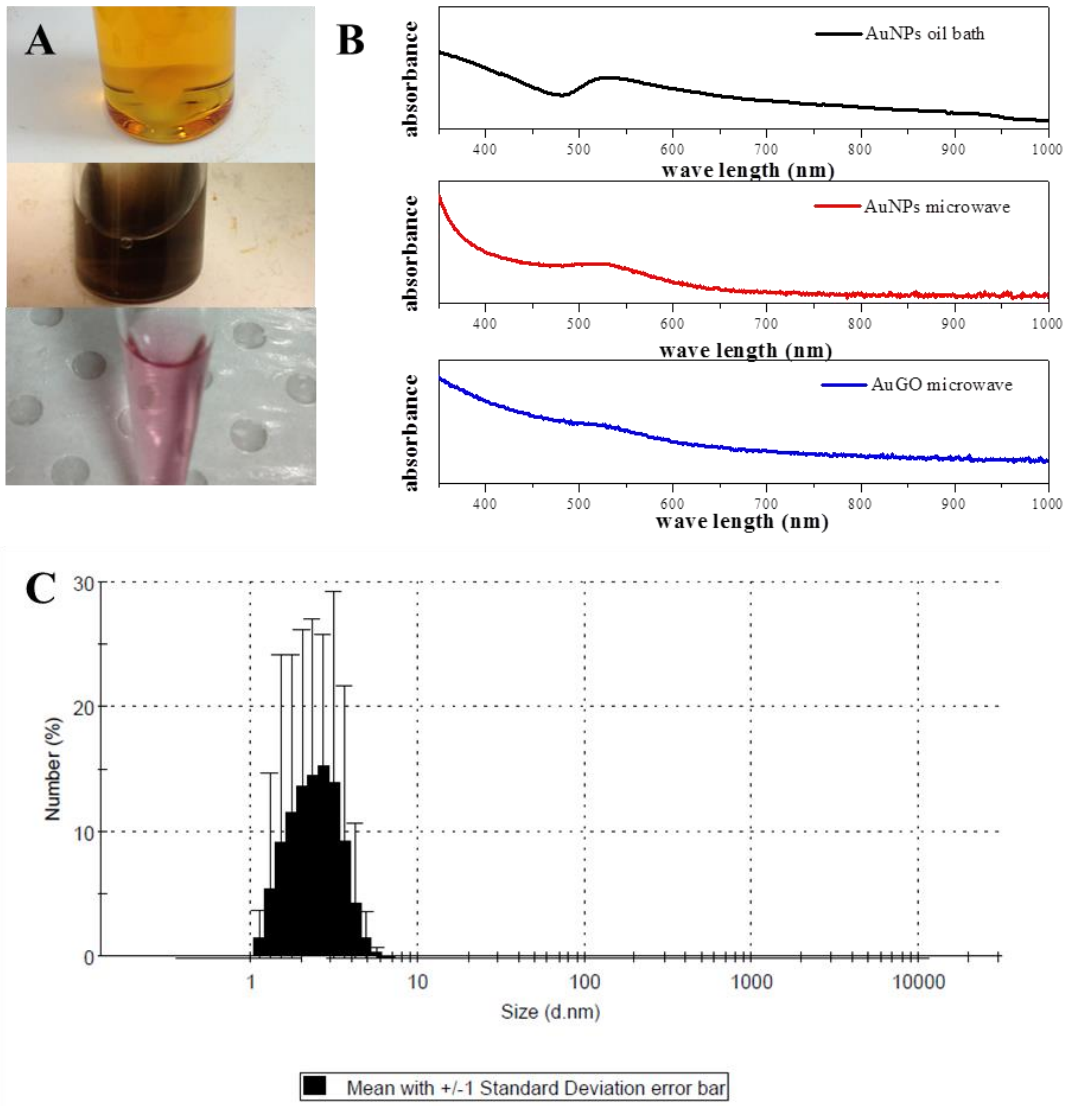

Figure 4.3: (A) Optical images for gold salt solutions (top) prior to, (middle) subsequent to be heated in oil bath, and (bottom) microwave irradiation; (B) Uv-vis analysis of AuNPs synthesized in oil bath for 16h and microwave for 1h and microwave synthesized AuGO for 1h; (C) Zeta sizer test of microwave synthetized AuNPs.

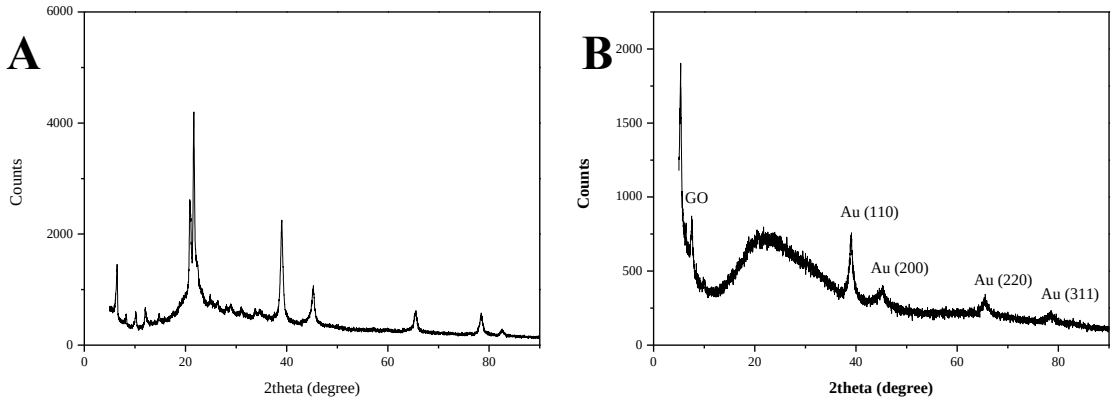

Figure 4.4: XRD of the oil bath (A) and microwave (B) synthetized AuGO.

The AuGO was synthesized by heating the solution containing graphene oxide sheets, $HAuCl_4$, ethanol, oleylamine and hexane for 16 h in 55 ℃ oil bath. A group of AuGO samples are prepared with a series ratio of Au/GO (16:1, 2:1, and 1:3) and heating time (8 h, 16 h, and 24 h). AuNPs decorated graphene oxide sheet was hypothesized to be facilitated by oleaylamine [20]. Au^{3+} is firstly reduced to Au^{+} and compounded with oleaylamine, and then the complex was adsorbed onto the GO which was dispersed in organic solvent with the assist of the long-chain alkylamine molecules, the complex self-organized into ordered supramolecular structures through aurophilic interactions [21, 22]. After heated at 55 ℃ for 8 h, no Au nanoparticles appeared on the GO surface (Figure 4.5A). The formation of Au seeds or particles is a slow process to reduce Au^{+}

from oleylamine–AuCl. The scanning electron microscopy of AuNPs decorated on graphene oxide demonstrated that the particles produced by this oil heating method were clearly deposited between the graphene oxide sheets (Figure 4.5). The flower cluster nanostructure was obtained at the high ratio of 16:1 Au/GO and it exhibited a size range from around 200 and 500 nm in SEM (Figure 4.5 B, C &D) and TEM (Figure 4.6A). The reducing $HAuCl_4$ concentration leaded to the decreasing amount of particles appearing on the defect sites as well as the smaller size.

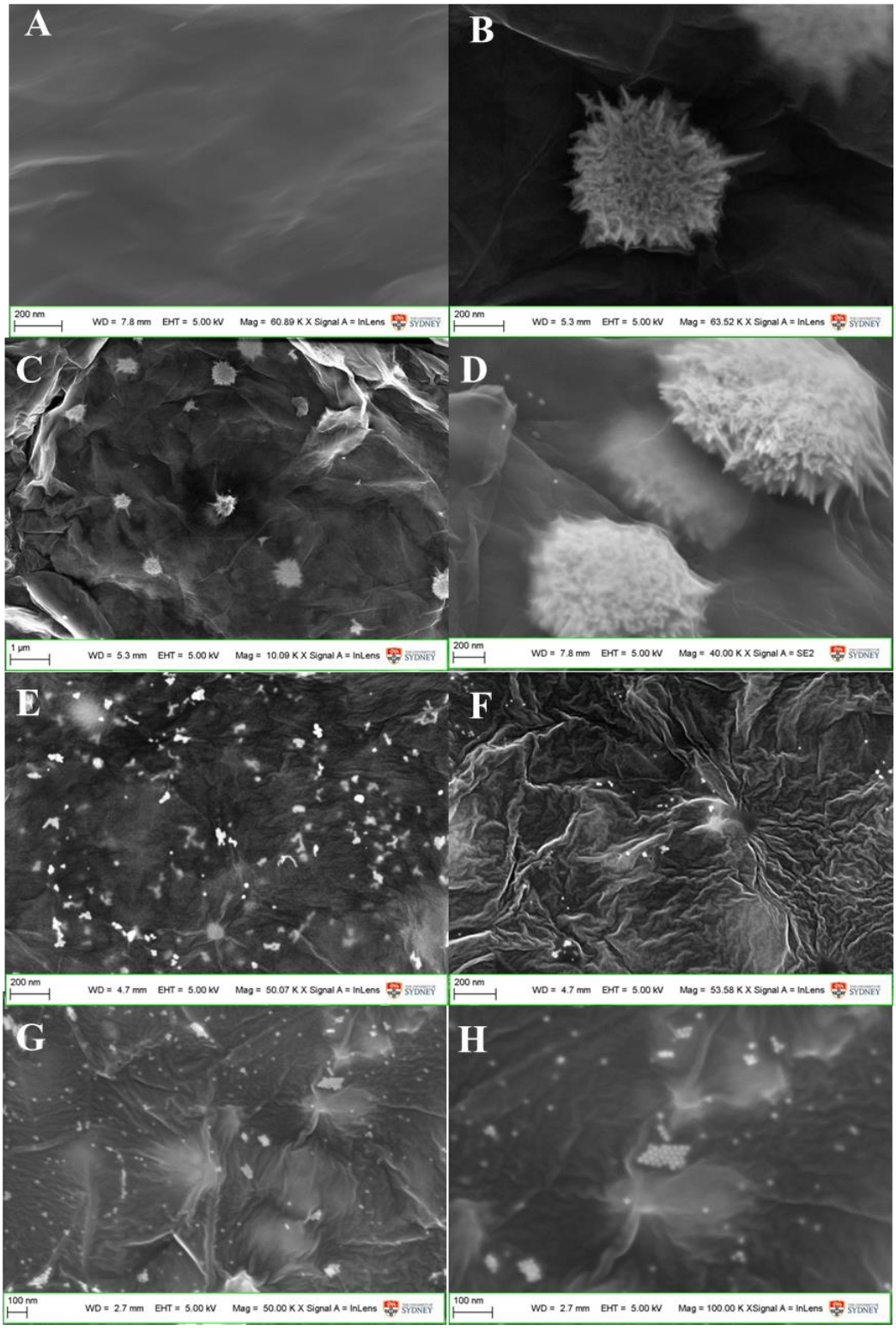
A
200 nm
WD = 7.8 mm EHT = 5.00 kV Mag = 60.89 K X Signal A = InLens
B
200 nm
WD = 5.3 mm EHT = 5.00 kV Mag = 63.52 K X Signal A = InLens
C
1 µm
WD = 5.3 mm EHT = 5.00 kV Mag = 10.09 K X Signal A = InLens
D
200 nm
WD = 7.8 mm EHT = 5.00 kV Mag = 40.00 K X Signal A = SE2
E
200 nm
WD = 4.7 mm EHT = 5.00 kV Mag = 50.07 K X Signal A = InLens
F
200 nm
WD = 4.7 mm EHT = 5.00 kV Mag = 53.58 K X Signal A = InLens
G
100 nm
WD = 2.7 mm EHT = 5.00 kV Mag = 50.00 K X Signal A = InLens
H
100 nm
WD = 2.7 mm EHT = 5.00 kV Mag = 100.00 K XSignal A = InLens

Figure 4.5: SEM images of the oil bath synthetized AuGO for 16 h with Au/GO ratio 16:1 (A&B), 2:1 (C) and 1:3 (D); the oil bath synthetized AuGO for 24 h (E) and 8 h (F) with Au/GO ratio 16:1; and microwave synthetized AuGO for 1h with Au/GO ratio 16:1 (G&H).

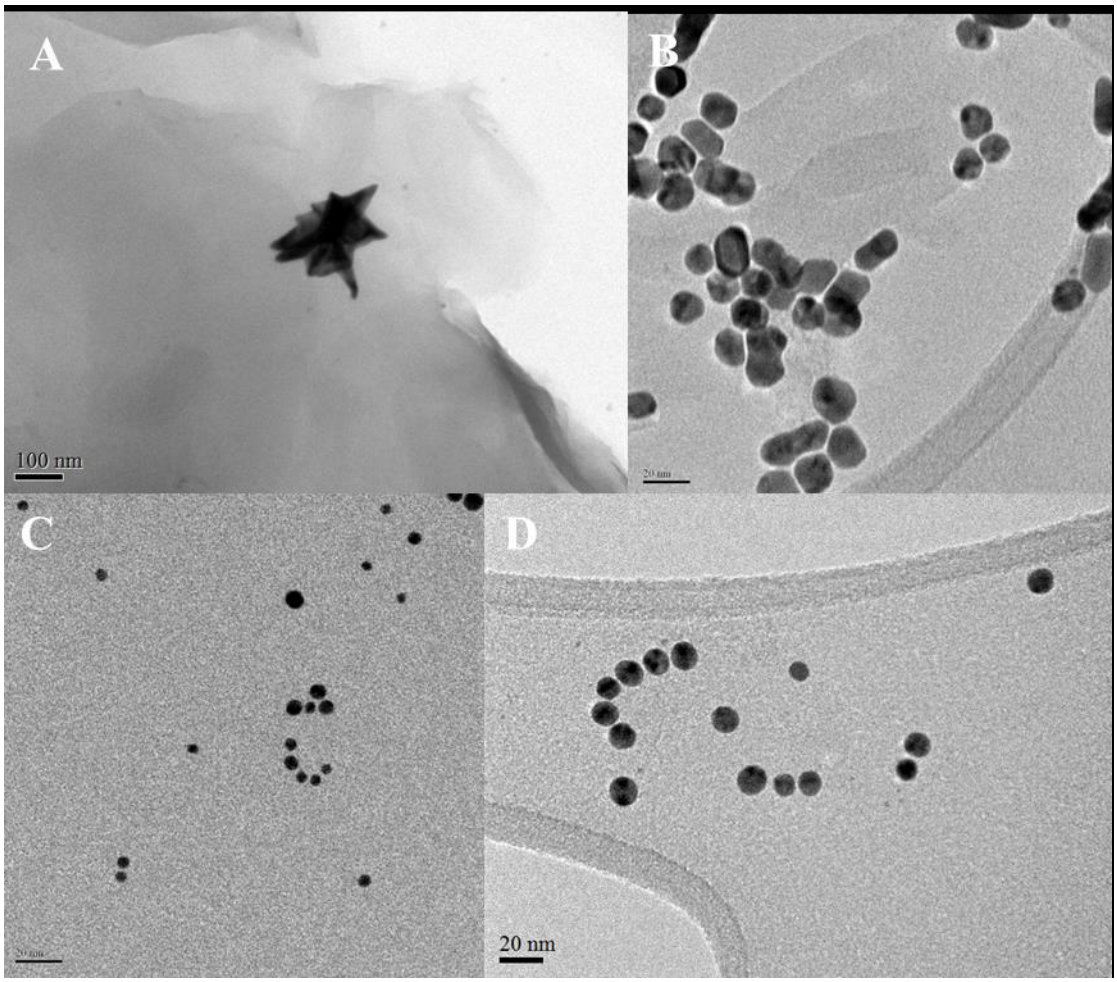

Figure 4.6: TEM images of the oil bath AuGO (A) and microwave synthetized AuNPs (B) and AuGO (C&D).

Microwave irradiation provides a convenient, safe and economic method and has been used to speed up a range of organic chemistry reactions [23, 24]. Microwave assisted AuGO synthesis is a very fast process and the electric energy can be directly transferred to the reactant regents with a rapid temperature increase. The AuNPs were produced when the mixture solution was heated in pressure vessel in a microwave oven for 1 h (Figure 4.5G&H and Figure 4.6C&D). In addition, the SEM and TEM provide clear evidence of a narrow size distribution (from around 8 nm to 14 nm) highlighting the reactivity of the radicals produced by this method.

4.3.2 Quantitative dopamine detection with AuGO/Fab' electrode

CV experiments were conducted to detect the electrochemical properties of the AuGO coated on the glassy carbon electrode as well as the antibody fragment loaded AuGO (Figure 4.7). In the CV curves, the double layer capacitance was always present and increased as the scan rate rose. The capacitive current flow is not related to redox reactions, it is therefore mostly regarded as "background current" to the reaction [25]. By comparing the electrodes with or without the presence of Fab', electrochemical current output at double-layer region decreased due to the Fab'. The induction of protein resulted in a significant rising of electrical resistance that was attributed to the combination of less effective charge transfer at the electrode interface and double layer capacitance within the catalyst layer. The application of both kinds of AuGO electrodes produced a Faradic response in deaerated 0.1M PBS as well as a double layer effect. In

the CV measurements of the AuGO/Fab' electrode, the presence of 100 μM DA in PBS was oxidised and generated responses at about 0.21 V *vs*. Ag/AgCl. The CVs clearly showed symmetric redox peaks that can be ascribed to the electron transfer-chemical reaction-electron transfer (ECE) mechanism of dopamine electrochemical oxidation.

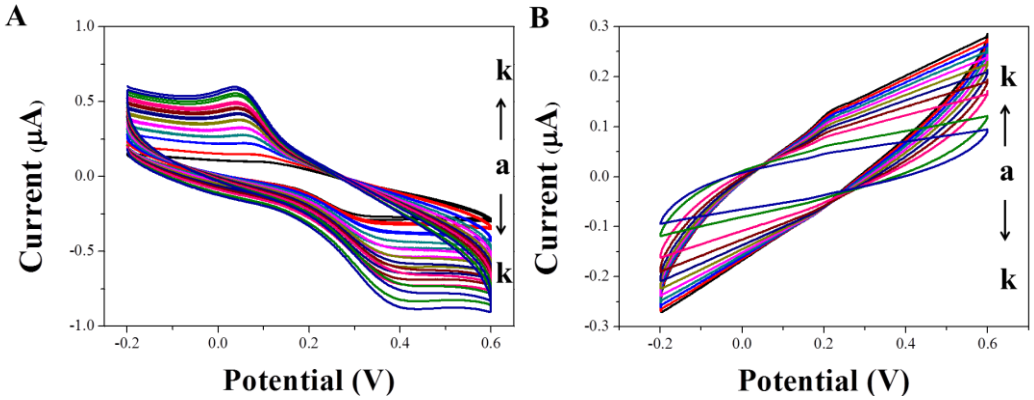

Figure 4.7: CV of the microwave assisted synthetized AuGO electrode (A) and AuGO/Fab' (B) in 100 μM DA solution (pH 7.0 PBS) at different scan rates (a-k): 10, 20, 40, 60, 80, 100, 120, 140, 160, 180 and 200 mV·s^{-1}.

The AuGO/Fab' electrode was utilized to determine dopamine in the pH 7.0 PBS solution. As shown in Figure 4.8, it can be seen that approximate 0.24 μA and 0.1 μA current was detected at 0.17 V vs Ag/AgCl for 100 μM and 10 μM DA, respectively. The DPV curves for 10 and 100 μM DA on AuGO electrode investigated signals from 0.04 to 0.5 V *vs*. Ag/AgCl with a peak at 0.25 V *vs*. Ag/AgCl. Both electrodes were able

to detect dopamine as low as 10 μM and in the case of 1 below μM, noise and instability have impacted on the determination. However, loading with the antibody decreased signal (i.e. *Ipa*), the I_{pa} for a 100 μM DA solution at the AuGO electrode (1.01 μA) was 4 times higher than that of AuGO/Fab' electrode under identical testing conditions. Fortunately, AuGO/Fab' showed an efficient oxidation with narrow respond distribution (0.09-0.26 V *vs*. Ag/AgCl), which demonstrated the trend of high selectivity.

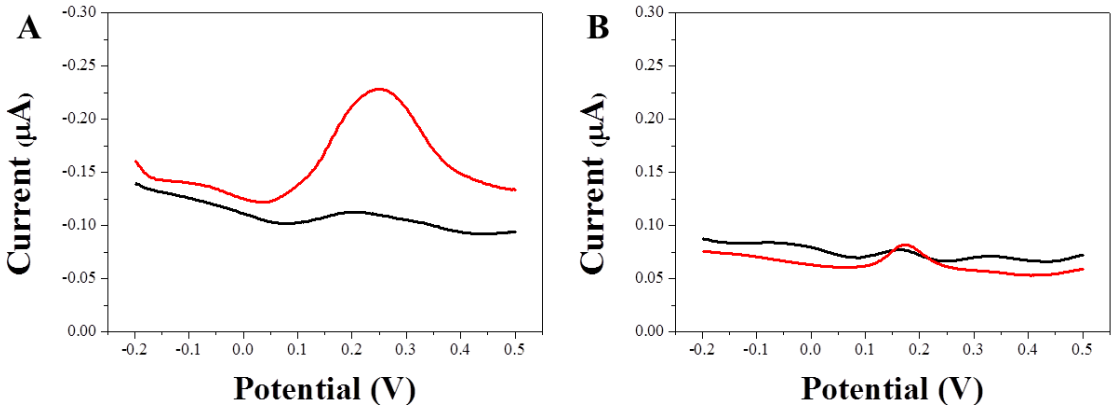

Figure 4.8: DPV of the microwave synthetized AuGO electrode (A) and AuGO-Fab' (B) in 10 (black) and 100 (red) μM DA solution (pH 7.0 PBS).

The aim of induction of antibody fragment is to develop a simple biorecognition molecular based analytical test which combines the great sensitivity immunoassays. It is hypothesized that electrochemical performance is enhanced, such as low limit of

detecting and increasing signals. Unfortunately, the AuGO/Fab' electrode does not show numerous improvements in the dopamine determination. The above demonstrated failure may be ascribed to two main reasons. The first one is the properties and amount of the antibody fragment on the AuGO surface. The pepsin digestion and 2-MEA cleaving were used to split the anti-dopamine antibody to useless Fc and Fab' which contained the specific targeting site of antibody and displayed similar specificity of the whole antibody [26]. Due to the limit of a chemistry lab, I did not conduct the analysis of the activity and amount of Fab' obtained, resulting in uncertain affinity of the immunoelectrode to the antigen. Secondly, low molecular weight target detection may be out of the sensitivity of the immunosensing [27]. The direct electrochemical immunosensor can detect the antibody-antigen complex formation by certain measurements. Antibody-antigen interaction leads to a change in surface properties which is sensed by potential and capacitance on the surface of the transducer. The limited change in mass of surface-immobilized species may significantly impact on the determination.

4.4 Conclusions and further study

In this chapter, anti-dopamine antibody fragmentation and immobilisation of Fab' fragment into the AuNPs/GO coated electrode was described. And the application of this immunosensor for substance detection was investigated in this study. The electrochemical properties of AuGO/Fab' were tested by CV and DPV. Although the

low limit of detecting was not reached, the Fab' loaded immunoelectrode narrowed the oxidation potential.

Further study will be conducted on obtaining the fragment in different conditions such as enzyme concentration, digestion time and so on. In addition, the analysis of the fragment affinity is proposed by western blot or ELISA. The whole antibody based immunosenor is in the future project as well.

4.5 References

1. Yalow, R.S. and S.A. Berson, *Assay of plasma insulin in human subjects by immunological methods.* 1959.

2. Engvall, E. and P. Perlmann, *Enzyme-linked immunosorbent assay (ELISA) quantitative assay of immunoglobulin G.* Immunochemistry, 1971. **8**(9): p. 871.

3. Sadik, O.A. and J.M. Van Emon, *Applications of electrochemical immunosensors to environmental monitoring.* Biosensors and Bioelectronics, 1996. **11**(8): p. i.

4. Kim, J.-I., A. Bordeanu, and J.-C. Pyun, *Diamond-like carbon (DLC) microelectrode for electrochemical ELISA.* Biosensors and Bioelectronics, 2009. **24**(5): p. 1394.

5. Ivnitski, D., et al., *Application of electrochemical biosensors for detection of food pathogenic bacteria.* Electroanalysis, 2000. **12**(5): p. 317.

6. Vallée-Bélisle, A., et al., *Bioelectrochemical switches for the quantitative detection of antibodies directly in whole blood.* Journal of the American Chemical Society, 2012. **134**(37): p. 15197.

7. Hock, B., *Antibodies for immunosensors a review.* Analytica Chimica Acta, 1997. **347**(1): p. 177.

8. Cosnier, S., *Affinity biosensors based on electropolymerized films.* Electroanalysis, 2005. **17**(19): p. 1701.

9. Díaz‐González, M., M.B. González‐García, and A. Costa‐García, *Recent advances in electrochemical enzyme immunoassays.* Electroanalysis, 2005. **17**(21): p. 1901.

10. Centi, S., S. Laschi, and M. Mascini, *Strategies for electrochemical detection in immunochemistry.* Bioanalysis, 2009. **1**(7): p. 1271.

11. Munge, B.S., et al., *Nanostructured Immunosensor for Attomolar Detection of Cancer Biomarker Interleukin‐8 Using Massively Labeled Superparamagnetic Particles.* Angewandte Chemie, 2011. **123**(34): p. 8061.

12. Holford, T.R., F. Davis, and S.P. Higson, *Recent trends in antibody based sensors.* Biosensors and Bioelectronics, 2012. **34**(1): p. 12.

13. Chai, R., et al., *Amperometric immunosensors based on layer-by-layer assembly of gold nanoparticles and methylene blue on thiourea modified glassy carbon electrode for determination of human chorionic gonadotrophin.* Talanta, 2008. **74**(5): p. 1330.

14. Mani, V., et al., *Ultrasensitive immunosensor for cancer biomarker proteins using gold nanoparticle film electrodes and multienzyme-particle amplification.* ACS nano, 2009. **3**(3): p. 585.

15. Holliger, P. and P.J. Hudson, *Engineered antibody fragments and the rise of single domains.* Nature biotechnology, 2005. **23**(9): p. 1126.

16. Hummers Jr, W.S. and R.E. Offeman, *Preparation of graphitic oxide.* Journal of the American Chemical Society, 1958. **80**(6): p. 1339.

17. Andrew, S.M. and J.A. Titus, *Fragmentation of immunoglobulin G.* Current Protocols in Cell Biology, 2003: p. 16.4. 1.

18. Kausaite-Minkstimiene, A., et al., *Comparative study of random and oriented antibody immobilization techniques on the binding capacity of immunosensor.* Analytical chemistry, 2010. **82**(15): p. 6401.

19. Amendola, V. and M. Meneghetti, *Size evaluation of gold nanoparticles by UV−vis spectroscopy.* The Journal of Physical Chemistry C, 2009. **113**(11): p. 4277.

20. Huang, X., et al., *Synthesis of hexagonal close-packed gold nanostructures.* Nature communications, 2011. **2**: p. 292.

21. Niyogi, S., et al., *Solution properties of graphite and graphene.* Journal of the American Chemical Society, 2006. **128**(24): p. 7720.

22. Schmidbaur, H. and A. Schier, *A briefing on aurophilicity.* Chemical Society Reviews, 2008. **37**(9): p. 1931.

23. Lidström, P., et al., *Microwave assisted organic synthesis—a review.* Tetrahedron, 2001. **57**(45): p. 9225.

24. Dahl, J.A., B.L. Maddux, and J.E. Hutchison, *Toward greener nanosynthesis.* Chemical reviews, 2007. **107**(6): p. 2228.

25. Harnisch, F. and S. Freguia, *A basic tutorial on cyclic voltammetry for the investigation of electroactive microbial biofilms.* Chemistry–An Asian Journal, 2012. **7**(3): p. 466.

26. Torrance, L., et al., *Oriented immobilisation of engineered single-chain antibodies to develop biosensors for virus detection.* Journal of virological methods, 2006. **134**(1): p. 164.

27. Ghindilis, A.L., et al., *Immunosensors: electrochemical sensing and other engineering approaches.* Biosensors and Bioelectronics, 1998. **13**(1): p. 113.